Circulation
JOURNAL OF THE AMERICAN HEART ASSOCIATION
American Heart Association®
Learn and Live℠

MicroRNA-24 Regulates Vascularity After Myocardial Infarction

Jan Fiedler, Virginija Jazbutyte, Bettina C. Kirchmaier, Shashi K. Gupta, Johan Lorenzen, Dorothee Hartmann, Paolo Galuppo, Susanne Kneitz, John T.G. Pena, Cherin Sohn-Lee, Xavier Loyer, Juergen Soutschek, Thomas Brand, Thomas Tuschl, Joerg Heineke, Ulrich Martin, Stefan Schulte-Merker, Georg Ertl, Stefan Engelhardt, Johann Bauersachs and Thomas Thum

Circulation 2011, 124:720-730: originally published online July 25, 2011
doi: 10.1161/CIRCULATIONAHA.111.039008
Circulation is published by the American Heart Association. 7272 Greenville Avenue, Dallas, TX 72514
Copyright © 2011 American Heart Association. All rights reserved. Print ISSN: 0009-7322. Online ISSN: 1524-4539

The online version of this article, along with updated information and services, is located on the World Wide Web at:
http://circ.ahajournals.org/content/124/6/720

Data Supplement (unedited) at:
http://circ.ahajournals.org/http://circ.ahajournals.org/content/suppl/2011/07/20/CIRCULATIONAHA.111.039008.DC1.html

Subscriptions: Information about subscribing to Circulation is online at
http://circ.ahajournals.org//subscriptions/

Permissions: Permissions & Rights Desk, Lippincott Williams & Wilkins, a division of Wolters Kluwer Health, 351 West Camden Street, Baltimore, MD 21202-2436. Phone: 410-528-4050. Fax: 410-528-8550. E-mail:
journalpermissions@lww.com

Reprints: Information about reprints can be found online at
http://www.lww.com/reprints

Downloaded from http://circ.ahajournals.org/ by guest on August 25, 2011

MicroRNA-24 Regulates Vascularity After Myocardial Infarction

Jan Fiedler, PhD; Virginija Jazbutyte, PhD; Bettina C. Kirchmaier, PhD; Shashi K. Gupta, MSc; Johan Lorenzen, MD; Dorothee Hartmann, MSc; Paolo Galuppo, PhD; Susanne Kneitz, PhD; John T.G. Pena, MD; Cherin Sohn-Lee, PhD; Xavier Loyer, PhD; Juergen Soutschek, PhD; Thomas Brand, PhD; Thomas Tuschl, PhD; Joerg Heineke, MD; Ulrich Martin, PhD; Stefan Schulte-Merker, PhD; Georg Ertl, MD; Stefan Engelhardt, MD, PhD; Johann Bauersachs, MD; Thomas Thum, MD, PhD

Background—Myocardial infarction leads to cardiac remodeling and development of heart failure. Insufficient myocardial capillary density after myocardial infarction has been identified as a critical event in this process, although the underlying mechanisms of cardiac angiogenesis are mechanistically not well understood.

Methods and Results—Here, we show that the small noncoding RNA microRNA-24 (miR-24) is enriched in cardiac endothelial cells and considerably upregulated after cardiac ischemia. MiR-24 induces endothelial cell apoptosis, abolishes endothelial capillary network formation on Matrigel, and inhibits cell sprouting from endothelial spheroids. These effects are mediated through targeting of the endothelium-enriched transcription factor GATA2 and the p21-activated kinase PAK4, which were identified by bioinformatic predictions and validated by luciferase gene reporter assays. Respective downstream signaling cascades involving phosphorylated BAD (Bcl-XL/Bcl-2–associated death promoter) and Sirtuin1 were identified by transcriptome, protein arrays, and chromatin immunoprecipitation analyses. Overexpression of miR-24 or silencing of its targets significantly impaired angiogenesis in zebrafish embryos. Blocking of endothelial miR-24 limited myocardial infarct size of mice via prevention of endothelial apoptosis and enhancement of vascularity, which led to preserved cardiac function and survival.

Conclusions—Our findings indicate that miR-24 acts as a critical regulator of endothelial cell apoptosis and angiogenesis and is suitable for therapeutic intervention in the setting of ischemic heart disease. **(*Circulation*. 2011;124:720-730.)**

Key Words: myocardial infarction ■ microRNAs ■ angiogenesis ■ antagomir ■ gene expression ■ heart failure

Myocardial infarction (MI) is a leading cause of morbidity and mortality worldwide. MI leads to scar formation and left ventricular remodeling, including cardiac dilatation, contractile dysfunction, cardiomyocyte hypertrophy, and fibrosis.[1] Tissue hypoxia triggers endothelial apoptosis, and insufficient capillary density further contributes to an increase of infarct size and left ventricular dysfunction.[2–4]

Clinical Perspective on p 730

MicroRNAs (miRNAs) are endogenous small noncoding RNA molecules that regulate a substantial fraction of the genome by binding to the 3′ untranslated region (3′UTR) of frequently coordinately acting target messenger RNAs.[5] MiRNAs have been identified as valuable therapeutic targets in a variety of diseases, including cardiovascular disease.[6–12] Inhibition of miRNA processing by genetic knockdown of Dicer expression impairs endothelial functions and angiogenesis.[13–15] Certain miRNAs are important regulators of endothelial function, especially angiogenesis.[7,13–17] A subset of miRNAs is regulated by tissue oxygen levels, and miR-24 is activated by hypoxic conditions via the hypoxia-inducible factor 1 (HIF-1).[18] Although miR-24 is expressed in a variety

Received April 19, 2011; accepted June 7, 2011.

From the Institute of Molecular and Translational Therapeutic Strategies (J.F., V.J., S.K.G., J.L., D.H., T. Thum), Department of Cardiology and Angiology (P.G., J.H., J.B.), and Leibniz Research Laboratories for Biotechnology and Artificial Organs (U.M.), Hannover Medical School, Hannover, Germany; Hubrecht Institute-KNAW and University Medical Centre, Utrecht, Netherlands (B.C.K., S.S.-M.); Cell and Developmental Biology, Biocenter (B.C.K., T.B.), and Interdisciplinary Center for Clinical Research, Microarray Core Facility (S.K.), University of Wuerzburg, Wuerzburg, Germany; Laboratory of RNA Molecular Biology, Rockefeller University, New York, NY (J.T.G.P., C.S.-L., T. Tuschl); Institute of Pharmacology and Toxicology, Technische Universitaet Muenchen, Muenchen, Germany (X.L., S.E.); Regulus Therapeutics, San Diego, CA (J.S.); National Heart and Lung Institute, Imperial College London, London, United Kingdom (T.B.); Department of Internal Medicine I, University Hospital Wuerzburg, Wuerzburg, Germany (G.E.); and Centre for Clinical and Basic Research, IRCCS San Raffaele, Rome, Italy (T. Thum).

The online-only Data Supplement is available with this article at http://circ.ahajournals.org/lookup/suppl/doi:10.1161/CIRCULATIONAHA.111.039008/-/DC1.

Correspondence to Thomas Thum, MD, PhD, Hannover Medical School, Institute for Molecular and Translational Therapeutic Strategies (IMTTS), OE8886, Carl Neuberg Strasse 1, 30625 Hannover, Germany. E-mail Thum.Thomas@mh-hannover.de

© 2011 American Heart Association, Inc.

Circulation **is available at http://circ.ahajournals.org** **DOI: 10.1161/CIRCULATIONAHA.111.039008**

Downloaded from http://circ.ahajournals.org/ by guest on August 25, 2011

of organs,[19] it is enriched in endothelial cells,[20] but its role in the cardiovascular system remains basically uncertain. Here, we show that miR-24 acts as a critical regulator of endothelial cell apoptosis and angiogenesis and is suitable for therapeutic intervention in the setting of ischemic heart disease.

Methods

miRNA/RNA Isolation, miRNA Reverse Transcription–Polymerase Chain Reaction, and Global Transcriptome Analysis

RNA isolation was performed with TRIzol reagent (Invitrogen) or the miRVana miRNA Isolation Kit (Ambion) according to the manufacturer's instructions. For detection of miRNAs in samples, different TaqMan miRNA assays (Applied Biosystems) were applied (online-only Data Supplement Table I). The small RNA molecule U6 small nuclear (Rnu6–2) was amplified as a control. Reverse transcription–polymerase chain reaction analysis was performed in an ICycler (Bio-Rad). To assess RNA integrity for downstream array analysis, total RNA was subjected to capillary chromatography in an Agilent bioanalyzer 2100. Gene array analysis was performed with the Affymetrix GeneChip system according to the manufacturer's instructions and with Human Gene 1.0ST arrays (Affymetrix Systems). Further microarray analyses and data handling were performed as described previously.[21]

Transfection Assays

Transient liposomal transfection of small inhibitory RNAs (siRNAs) or miRNAs was performed according to the manufacturers' instructions. Briefly, cells were split 1 day before transfection to reach 60% to 70% confluence on the day of transfection. Specific siRNAs/miRNAs and control siRNA/miRNA and Lipofectamine 2000 (Invitrogen) were mixed separately and incubated for 5 minutes with Opti-MEM I media (Invitrogen). Complexes were added together and incubated for 20 minutes. Media were changed to antibiotic-free media before the addition of liposomal siRNA complexes (final concentration 150 nmol/L for siRNA and 100 nmol/L for miRNAs). Cells were incubated for 4 hours before the media were changed to fresh media. Silencing of proteins or miRNA targets was monitored for 48 hours (siRNA) or 72 hours (miRNAs) after transfection by Western blot analysis. Specific details about the siRNAs and miRNAs used are given in Table II in the online-only Data Supplement.

Apoptosis Detection

Apoptosis was measured with the Annexin-V-Fluos kit from Roche Diagnostics (Penzberg, Germany) according to the manufacturer's instructions and as described previously.[6] Detection of apoptosis was either done by fluorescent-activated cell sorter analysis on a FACSCalibur (BD Biosciences) or by terminal deoxynucleotidyl transferase-mediated dUTP nick-end labeling (TUNEL) assays.

Western Blotting and ELISA

Western blot analysis was performed with 10 to 40 μg of total protein. Protein was blotted onto polyvinylidene fluoride membrane in Mini Trans-Blot electrophoretic transfer cell (Bio-Rad). Afterward, different antigens were detected by appropriate antibodies (online-only Data Supplement Table III). For phosphorylated Bcl-XL/Bcl-2–associated death promoter (phospho-BAD; Ser112) detection in cell culture samples, we applied a PathScan phospho-BAD (Ser112) sandwich ELISA kit (No. 7182; Cell Signaling) according to the manufacturer's instructions. Phospho-BAD levels were related to total BAD expression levels as obtained by Western blotting.

Analysis of Capillary and Arteriolar Density

Analyses of capillary and arteriolar density were performed in transverse sections of the periinfarct zone and the remote zone from left ventricles 14 days after MI. Capillary and arteriolar densities were evaluated after fluorescent immunohistochemical staining for platelet and endothelial cell adhesion molecule-1 (PECAM-1; endothelial marker) or α-smooth muscle actin (Acta2; smooth muscle cells) with antibodies listed in online-only Data Supplement Table III. Arterioles were recognized as vessels with 1 or more continuous layer of $Acta2^+$ vascular smooth muscle cells. The number of capillaries and arterioles per square millimeter was counted in a blinded fashion.

Tube Formation and Spheroid Formation Assay

Transfection or transduction of cultured cells was performed as mentioned previously. Then, cells were harvested and 15 000 cells were seeded on top of Matrigel-coated chamber slides (BD). After 6 to 8 hours and 24 hours, pictures were taken on a Zeiss AxioVision microscope (Jena, Germany). In selected experiments, a pan-caspase inhibitor (caspase 3 inhibitor I; Calbiochem; 100 μmol/L, 72 hours) was used. For spheroid formation, miRNA-transfected human umbilical vein endothelial cells were trypsinized and collected in EBM-2 medium containing FCS and 20% Methocel (Sigma-Aldrich). 500 cells in 100 μl of medium were plated per well in a 96-well plate (U-shaped bottom) and cultivated overnight at 37°C, 5% CO_2. The next day, spheroid formation was visualized by microscopy on a Nikon ECLIPSE Ti at 10× or 20× magnification. Spheroids were harvested at 200*g* and resuspended in a mixture of 80% Methocel and 20% FCS. Next, 50 spheroids per well were distributed in a 24-well plate by taking 500 μL of spheroid suspension together with 500 μL of collagen-containing matrix (DMEM, collagen solution, and NaOH). After 30 minutes' incubation at 37°C, 100 μL of EBM-2 medium supplemented with 40% FCS and basic fibroblast growth factor (30 ng/mL) was given on top of casted gels. Twenty-four hours after initial seeding, endothelial sprouts were fixed with 10% paraformaldehyde before sprouting capacity was evaluated by microscopy.

Scratch Wound (Migration) Assay

Transfected human umbilical vein endothelial cells were cultivated in EBM-2 medium at 37°C, 5% CO_2. The scratches in the cell monolayer were generated with a 100-μL tip, and the cells were photographed at 0, 8, and 24 hours with a Zeiss Axiovert 135 microscope. Subsequently, the distance between cell fronts was measured with an AxioVision documentation system (Zeiss).

Proliferation Assays

To measure proliferative capacity in miRNA-modulated cells, a WST-1 (Roche) or standard bromodeoxyuridine proliferation assay (Calbiochem) was applied. MiRNA transfection was performed as mentioned under Transfection Assays. Next, medium was changed and replaced by WST-1 or bromodeoxyuridine reagent as instructed by the manufacturer. WST-1 and bromodeoxyuridine absorbances were measured at 450 and 340 nm, respectively.

Luciferase Reporter Assays

A luciferase reporter assay system was applied to validate potential miRNA targets as described previously.[6] A putative 3′UTR miRNA binding sequence was cloned into the *Spe*I and *Hind*III cloning site of pMIR-REPORT vector (Ambion). Mutations in the putative miR-24 binding sites were introduced by site-directed mutagenesis (Quick Change II–Site-Directed Mutagenesis Kit; Stratagene). The mutations within the 3′UTRs were as follows (8-mer/7mer-8m seed in bold, mutated nucleotides underlined): GATA2 wild-type: 5′-CAGGCTGGG**CTGAGCCA**AAGCCAGAGTG-3′, GATA2 mutant 5′-CAGGCTGGG**CTGGTACA**AAGCCAGAGTG-3′; PAK4 wild-type 5′-CCTCTCCCC**CTGAGCCA**TTGGGGGGGTC-3′, PAK4 mutant 5′-CCTCTCCCC**CTGCTCCA**TTGGGGGGGTC-3′; RASA1 wild-type: 5′-TTAACAACCT**CTGAGCC**TTGGTGTA CAG-3′, RASA1 mutant 5′-TTAACAACCT**CTGGACC**TTGGTGTA CAG-3′; H2AFX wild-type (2 sites): 5′-CTGGA**CTGAGCC**TC … TG TATGCTAT**CTGAGCC**GTCT-3′.

The resulting construct was cotransfected with the miRNAs of interest and a β-galactosidase control plasmid (Promega) into HEK293 reporter cells in 48-well plates by use of Lipofectamine

Downloaded from http://circ.ahajournals.org/ by guest on August 25, 2011

2000 (Invitrogen). A total of 0.2 μg of plasmid DNA and 100 nmol/L miRNA was applied. Cells were incubated for 24 hours before luciferase and β-galactosidase activity was measured (Promega).

Chromatin Immunoprecipitation

Chromatin immunoprecipitation (ChIP) was used to detect protein-DNA interactions. We applied a ChIP protocol from Weinmann et al[22] with modifications and bioinformatic predictions[23, 24] as detailed in the online-only Data Supplement. The oligonucleotide primer sequences used are given in online-only Data Supplement Table IV.

Viral Transduction

The original green fluorescent protein (GFP)–murine-GATA2 plasmid was a gift from Marjo Simonen (Novartis, Basel, Switzerland). N-terminal GFP-tagged GATA2 was subcloned in an appropriate adenoviral entry vector. Adenoviruses were generated with the Gateway system (Invitrogen) by polymerase chain reaction amplification of the human cDNA sequence and recombination into the pAd/CMV/V5 destination vector (Invitrogen). Subsequently, 15 μg of purified recombinant adenoviral DNA was digested with PacI and precipitated with sodium acetate. One microgram of linearized vector was transfected to HEK 293 cells (Invitrogen) with Effectene reagent (Qiagen). After 3 amplifications, adenoviruses were purified and titrated with the Adeno-X Maxi purification kit and rapid titer kit (Clontech). For viral transduction experiments, cells were grown to subconfluence and infected with viral particles for 4 hours before the medium was changed. The multiplicity of infection was 4 to 40. A yellow fluorescent protein control virus was also applied with same multiplicity of infection.

In Vivo Studies

The studies conformed to the *Guide for the Care and Use of Laboratory Animals* published by the US National Institutes of Health (NIH publication No. 85-23, revised 1996).

Zebrafish Assays

Zebrafish wild-type TU and TL lines and the transgenic line *Tg(kdrl:eGFP)*^{s843} were kept at 28.5°C and staged as described previously.[25] To inhibit pigmentation, 0.003% 1-phenyl-2-thiourea was added to the embryo medium. Embryos were injected at the 1- to 2-cell stage with 2 nL of pre-miR-24 (25 μmol/L) or control pre-miRs (25 μmol/L). Injected embryos were analyzed 48 hours after fertilization (hpf). Images of living embryos were acquired with Leica MZ FLIII or Olympus SZX16 microscopes.

Morpholino-modified oligomers (MOs) were obtained from Gene Tools, LLC (Philomath, OR) and diluted in water containing 0.2% phenol red. Morpholino sequences are listed in online-only Data Supplement Table V. For control purposes, a standard control MO oligomer (MO-control; Gene Tools) was injected at the same concentration as a negative control. One- to 2-cell stage embryos were injected with previously validated 0.2 mmol/L MO1-gata2a[26] or 0.4 mmol/L MO2-gata2a.[27] In the case of *pak4*, morpholinos were designed against the ATG (MO1-pak4) and the fifth exon/intron boundary (MO2-pak4). One- to 2-cell stage embryos were injected with 2 to 4 ng of MO1-pak4 or 4 to 8 ng of MO2-pak4, respectively. Morpholino knockdown efficiency for start-site–targeting morpholinos was tested as recommended before by an in vivo translation-blockage assay. For the splice-site–targeting morpholino, MO2-pak4 knockdown efficiency was tested by RNA isolation from morpholino-injected zebrafish with TRIzol (Invitrogen) and subsequent cDNA from DNase-treated total RNA with M-MLV (Moloney murine leukemia virus) reverse transcriptase (Promega). Primers used for reverse transcriptase polymerase chain reactions are available on request.

For confocal analyses, zebrafish embryos were fixed at 48 hpf in a 4% paraformaldehyde solution overnight and embedded in 1.5% low melting point agarose. Confocal images were obtained with a Leica TCS SP2 confocal laser scanning microscope. The maximum projection algorithm of the Leica software was then used to calculate information sectored in different ranks to a 2-dimensional projection.

Myocardial Infarction

Male mice (*C57BL/6*, 8 to 10 weeks old) underwent coronary artery ligation for the production of MI as described previously.[28] Cardiac dimensions and function were analyzed by pulse-wave Doppler echocardiography essentially as described previously.[29] Further details are given in the online-only Data Supplement.

Statistical Analysis

Average data are presented as mean and SEM unless otherwise stated. Statistical analysis was performed with the StatView (SAS Institute) package. For statistical comparison of 2 groups, we used an unpaired 2-tailed Student *t* test; for the comparison of 3 or more groups, we used ANOVA followed by Bonferroni post hoc test. Differences were considered significant when $P<0.05$. In the Figures, probability values are indicated by 1 ($P<0.05$), 2 ($P<0.01$), or 3 ($P<0.005$) asterisks.

Please see the online-only Data Supplement for further details of the methods and materials used.

Results

MiR-24 Is Upregulated in Endothelial Cells by Cardiac Ischemia

A spatiotemporal analysis of miR-24 expression in fractionated cardiac cell types demonstrated selectively strong induction of miR-24 in endothelial cells isolated from ischemic but not remote myocardium early after MI (Figure 1A). Accordingly, costaining of mouse cardiac MI sections after in situ hybridization with fluorescein isothiocyanate–conjugated anti-miR-24 probes with cell-type–specific antibodies demonstrated specific enriched endothelial but not smooth muscle cell miR-24 expression in infarcted cardiac areas (Figures 1B and C). The hybridization signal was abolished when a hybridization probe with similar melting temperature but targeted against a scrambled sequence was used (data not shown). In line with the in situ hybridization experiments after ischemic cardiac injury, hypoxic culture conditions increased miR-24 expression in endothelial cells (Figure 1D).

MiR-24 Triggers Endothelial Apoptosis and Impairs Angiogenesis

To characterize miR-24 function, we overexpressed synthetic miR-24 precursors in human umbilical vein endothelial cells. MiR-24 overexpression induced apoptosis in endothelial cells, whereas miR-24 antagonism reduced apoptosis (Figure 2A). Hypoxia-induced apoptosis of endothelial cells was attenuated by blocking endogenous miR-24, whereas overexpression of miR-24 with synthetic precursors exaggerated endothelial apoptosis (Figure 2B). MiR-24 attenuated tube formation (−81%; $P<0.0001$) independently from its pro-apoptotic effects, which suggests the potential involvement of multiple target networks (Figure 2C; online-only Data Supplement Figure Ia). Endothelial spheroid formation, sprouting capacity, migration in scratch wound assays, and proliferation were also impaired by miR-24 (Figures 2C through 2E).

GATA2 and PAK4 Are Targets of miR-24

To identify miR-24 targets that trigger endothelial apoptosis and impair angiogenic properties, we first used bioinformatics miRNA target prediction tools and detected a substantial number of genes with putative 3′UTR binding sites for miR-24 that encompassed important functional roles in en-

Downloaded from http://circ.ahajournals.org/ by guest on August 25, 2011

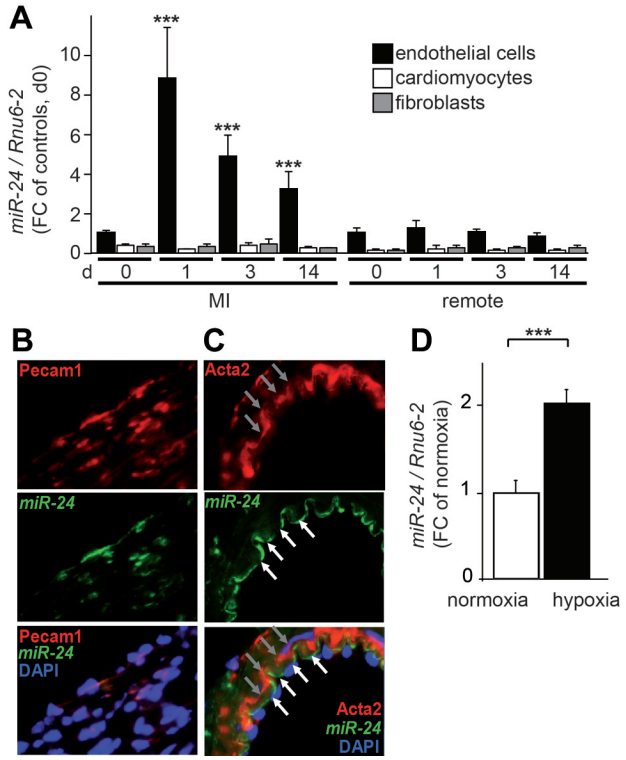

Figure 1. Selective miR-24 upregulation in endothelial cells after myocardial infarction (MI). **A**, Expression of miR-24 relative to Rnu6–2 in fractionated endothelial cells (magnetic affinity cell-sorted CD146$^+$ cells), cardiac fibroblasts, and cardiomyocytes of the periinfarct (MI) or remote region 0, 1, 3, or 14 days after MI in mice. In situ hybridization of *miR-24* with fluorescent probes and costaining against (**B**) endothelial (platelet and endothelial cell adhesion molecule-1 [Pecam1]) and (**C**) smooth muscle cell (Acta2) markers in mice after MI. **D**, Expression of *miR-24/RNU6–2* in human umbilical vein endothelial cells 24 hours after normoxic (21% O_2) or hypoxic conditions (1% O_2). n=3 to 7 per experiments or animals per group. Data are mean and SEM; *P<0.05, ***P<0.005. FC indicates fold change.

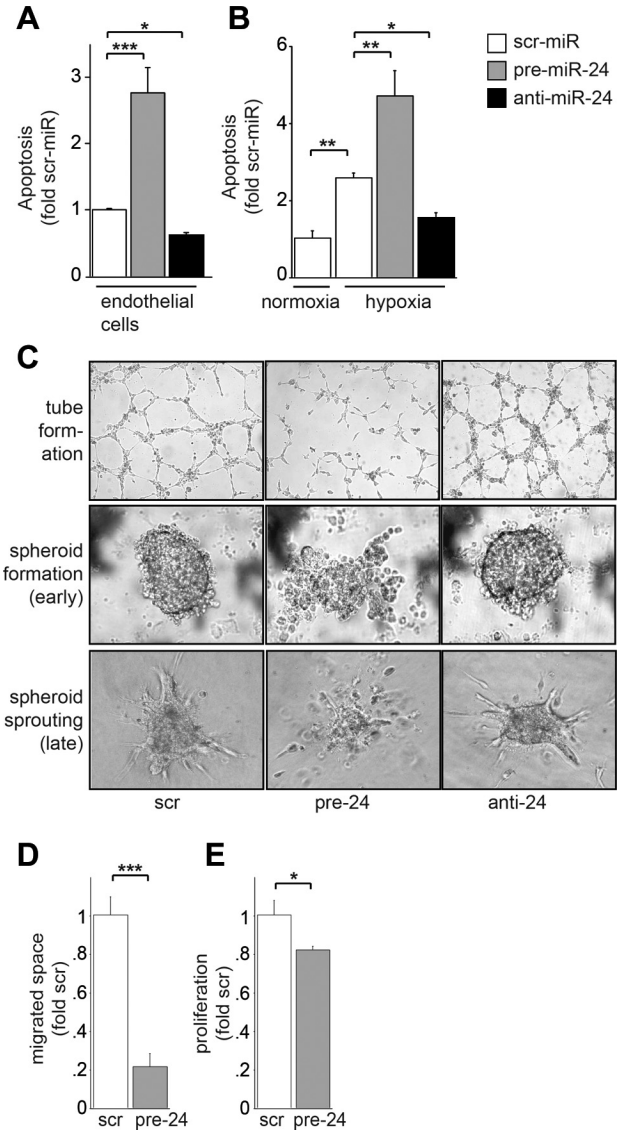

Figure 2. Activation of endothelial apoptotic programs and impairment of angiogenic properties by miR-24. **A**, Relative changes of apoptotic cells 72 hours after transfection of human umbilical vein endothelial cells with scrambled-miR (scr), synthetic mir-24 precursors (pre-24), or miR-24 antagonists (anti-24). **B**, Changes of apoptotic endothelial cells after transfection with scr-miR, pre-miR-24, or anti-miR-24 for 72 hours and subsequent exposure to hypoxia (1% O_2, 24 hours) or normoxia (21% O_2, 24 hours). **C**, Tube formation (top), spheroid formation (middle), and sprouting (bottom) capacity of human umbilical vein endothelial cells 72 hours after transfection with scr-miR, pre-miR-24, or anti-miR-24. **D** and **E**, Migratory (scratch wound assay; **D**) and proliferation (bromodeoxyuridine assay; **E**) capacity of human umbilical vein endothelial cells 72 hours after transfection with miR-24 or scrambled controls. n=3 to 4 experiments per group. Data are mean and SEM; *P<0.05, **P<0.01,***P<0.005.

dothelium (Table[30–42]). Of major interest were the transcription factor *GATA2* and the p21-activated kinase *PAK4*, both of which have established roles in vascular biology.[30,43,44] To validate those targets, primary endothelial cells were first transfected with miR-24 precursors. This resulted in repression of GATA2 and PAK4 protein expression. PAK4 was additionally repressed at the mRNA level (Figure 3A and data not shown). Inhibition of miR-24 in endothelial cells by specific antagonists increased GATA2 and PAK4 expression (data not shown).

When we fused the respective 3′UTR regions to a luciferase reporter gene and determined luciferase activity in cells transfected with synthetic miR-24 precursors, miR-24 significantly repressed luciferase activity, whereas unrelated miRNAs showed no effect (Figure 3B). We thus identified *GATA2* and *PAK4* as direct targets of miR-24. Bioinformatic miR-24 target prediction identified further potential targets (Table). We also validated the RAS p21 protein activator *RASA1* and the histone coding gene *H2AFX*, because of its described role in tumor vascularization.[35] Overexpression of miR-24 in endothelial cells reduced RASA1 and H2AFX protein expression, and luciferase gene reporter assays identified them as direct miR-24 targets (online-only Data Supplement Figures IIa and IIb). Functionally, RASA1 silencing induced modest endothelial apoptosis but did not alter tube formation, whereas no effects were seen after H2AFX downregulation (online-only Data Supplement Figures IIc through IIe). In strong contrast, silencing of both GATA2 and PAK4 in endothelial cells by siRNA abrogated tube formation

Downloaded from http://circ.ahajournals.org/ by guest on August 25, 2011

Table. Predicted microRNA-24 Target Messenger RNAs

Gene Symbol	Gene Name	Endothelial Expression Observed (Reference)	Evolutionary Conserved No. of Species (miRBase)	Predicted Target (miRBase)	Predicted Target (PicTar)	Seed Match for *miR-24* (TargetScan)
GATA2	Endothelial transcription factor GATA2	30	4	Yes	No	8mer
PAK4	Serine/threonine-protein kinase PAK4	31	5	No	Yes	8mer
RASA1	Ras GTPase-activating protein 1	32	10	No	Yes	8mer
CDKN1B	Cyclin-dependent kinase inhibitor 1B (p27Kip1)	33	4	No	Yes	8mer
AMOTL2	Angiomotin like 2	34	3	No	Yes	8mer
H2AFX	Histone family, member X	35	5	Yes	Yes	7mer
RAP1B	RAP1B, member of RAS oncogene family	36	5	No	Yes	8mer
AXL	AXL receptor tyrosine kinase	37	8	No	Yes	7mer
S1PR1	Sphingosine-1-phosphate receptor 1	38	NA	NA	NA	8mer
MAGI1	Membrane associated guanylate kinase, WW and PDZ domain containing 1	39	5	No	NA	8mer
TFPI	Tissue factor pathway inhibitor	40	5	No	NA	8mer
ANGPT4	Angiopoietin 4	41	5	No	NA	8mer
BMPR2	Protein receptor, type II	42	6	No	No	7mer

The microRNA databases and target prediction tools miRBase (http://microrna.sanger.ac.uk/), PicTar (http://pictar.mdc-berlin.de/), and TargetScan (http://www.targetscan.org/index.html) were used to identify potential microRNA-24 targets. NA indicates not available.

capacity and significantly induced apoptosis (Figures 3C and 3D). Immunohistochemical and Western blotting analyses revealed enriched cardiac endothelial expression of GATA2, PAK4, and RASA1 (online-only Data Supplement Figures IIIa and IIIb), which suggests cell-type specific coexpression of miR-24 with those targets within the heart.

Downstream GATA2 and PAK4 Target Regulation

To understand the observed cellular changes in miR-24 target regulation, we further investigated the downstream signaling cascades of the direct miR-24 targets GATA2 and PAK4. First, we used a global transcriptome analysis after viral overexpression or silencing of GATA2 in endothelial cells

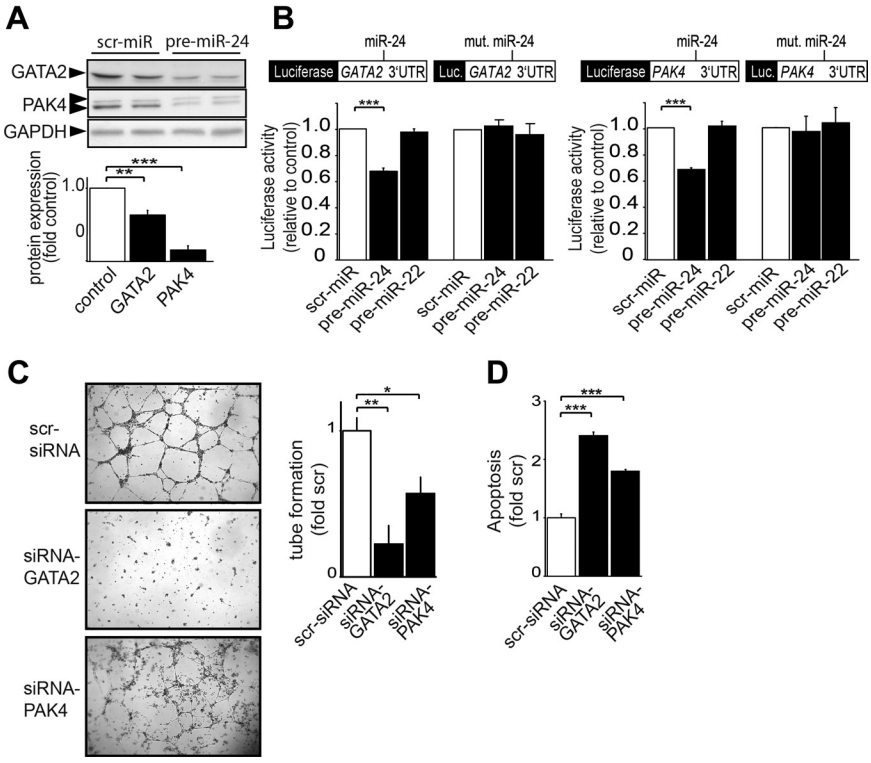

Figure 3. MiR-24 regulates GATA2 and PAK4 in endothelial cells. **A**, Protein expression of GATA2, PAK4, and GAPDH 72 hours after transfection with scrambled miRNAs (scr-miR) or synthetic miR-24 precursors (pre-miR-24) to human umbilical vein endothelial cells and statistical summary. **B**, Activities of luciferase reporter constructs comprising the 3′UTR regions of *GATA2* and *PAK4* mRNA relative to β-Gal control plasmids after transfection of synthetic miRNAs. mut indicates mutant. **C**, Tube formation of HUVECs after transfection of scrambled small inhibitory RNA (scr-siRNA) or siRNA against *GATA2* or *PAK4* 24 hours after seeding on top of Matrigels and statistical analysis. **D**, Apoptosis of endothelial cells after transfection of scrambled siRNA (scr-siRNA) or siRNAs specific for *GATA2* (siRNA-GATA2) or *PAK4* (siRNA-PAK4). Data are mean and SEM; $^{*}P<0.05$, $^{**}P<0.01$,$^{***}P<0.005$.

Downloaded from http://circ.ahajournals.org/ by guest on August 25, 2011

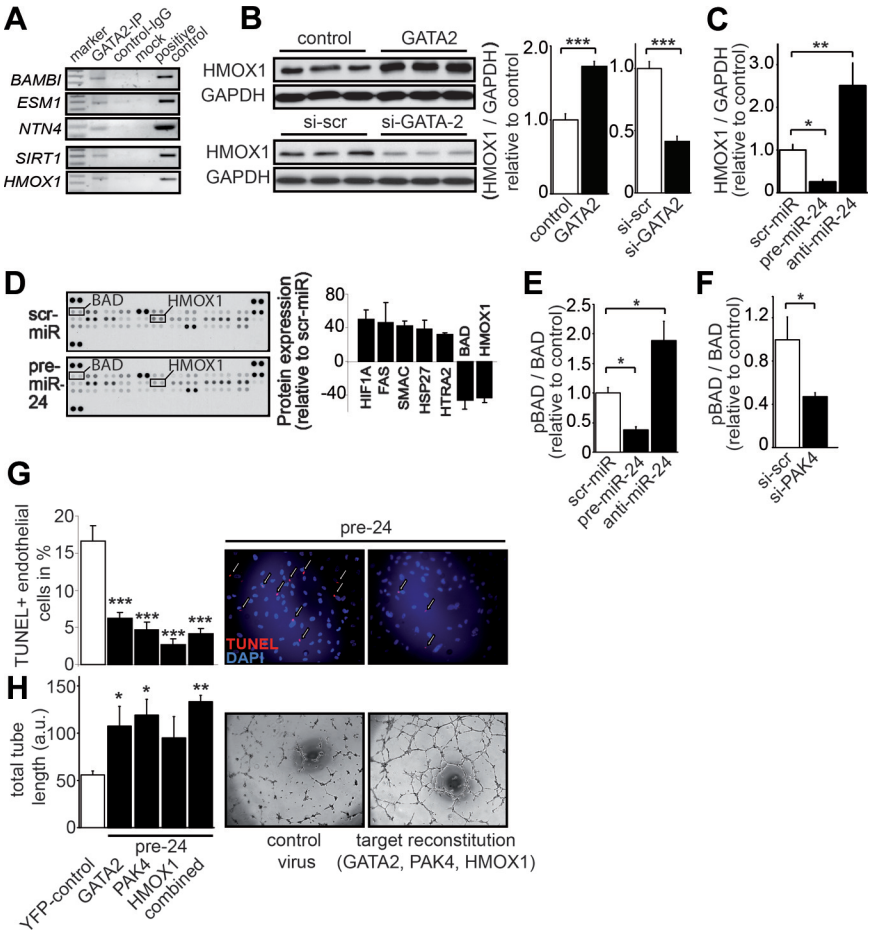

Figure 4. GATA2, PAK4, and their downstream targets are involved in the action of miR-24 in endothelial cells. **A**, Chromatin immunoprecipitation of several DNA sequences by GATA2 (GATA2-IP) compared with appropriate controls. **B**, Heme oxygenase 1 (HMOX1, left) expression in endothelial cells after GATA2 or (**C**) miR-24 modulation. **D**, Signal intensity of 35 different apoptosis-related proteins (in duplicates) on Proteome Profiler Array membranes (left) and statistical summary (right) after hybridization of endothelial protein extracts 72 hours after transfection with scrambled-miRNAs (scr-miR) or synthetic miR-24 precursors (pre-miR-24). **E**, Ratio of phospho-BAD (Bcl-XL/Bcl-2–associated death promoter; measured by ELISA) relative to BAD expression (measured by Western blot) in endothelial cells 72 hours after transfection with scr-miR, pre-miR-24, or anti-miR-24. **F**, pBAD/BAD ratio in endothelial cells 48 hours after transfection of scrambled siRNA (scr-siRNA) or siRNA against *PAK4* (siRNA-PAK4). si-scr indicates scrambled siRNA. **G**, TUNEL assay was used to detect apoptotic cells and (**H**) total endothelial tube length 48 hours after transfection of miR-24 precursors (pre-24) to pre-transfected (24 hours; yellow fluorescent protein [YFP] control construct, GATA2-, PAK4, and/or HMOX-1 construct; each miR-24-resistant) human endothelial cells. a.u. indicates arbitrary units. n=3 to 6 experiments per group. Data are mean and SEM; $^{*}P<0.05$, $^{**}P<0.01$, $^{***}P<0.005$.

(online-only Data Supplement Figures IVa and IVb and data not shown) and identified 3 reciprocally regulated mRNAs after GATA2 modulation (BMP and activin membrane-bound inhibitor [BAMBI], endothelial cell–specific molecule-1 [ESM1], and netrin-4 [NTN4]). Bioinformatics studies identified BAMBI, ESM1, NTN4, heme-oxygenase-1 (HMOX1), and sirtuin-1 (SIRT1) as harboring GATA2 binding sites within their promoter sequence (data not shown). To further validate GATA2-mediated regulation, we used GATA2-ChIP and found those 5 mRNAs to be highly enriched after ChIP (Figure 4A). GATA2 overexpression strongly induced protein expression of SIRT1 and HMOX1 (both of which play important roles in angiogenesis[45,46]), whereas siRNA-mediated GATA2 silencing reduced expression (Figure 4B; online-only Data Supplement Figures IVc and IVd). HMOX1 was regulated by miR-24 via modulation of GATA2 (Figure 4C; online-only Data Supplement Figures Va and Vb). HMOX1 exerts vasoprotective and antiapoptotic actions in endothelial cells,[46] and consequently, we found miR-24–mediated repression of HMOX1 resulted in enhanced reactive oxygen species formation in endothelial cells (online-only Data Supplement Figure Vc), which may also contribute to recent findings that miR-24 upregulation predisposes cells to DNA damage.[47]

To identify proteins that further mediated the proapoptotic action of endothelial miR-24, we hybridized endothelial protein extracts after transfection of scrambled miRs or synthetic miR-24 precursors to a protein microarray spotted with antibodies for proteins involved in apoptosis (Figure 4D). A number of proapoptotic proteins were upregulated, eg, HIF-1α (HIF-1a) and FAS, although we found a strong reduction of BAD and HMOX1 (Figures 4C through 4E). The direct miR-24 target PAK4 promotes BAD phosphorylation, thus inactivating the proapoptotic protein BAD.[48] MiR-24 overexpression led to a reduction of phosphorylated BAD (pBAD), whereas miR-24 antagonism increased the pBAD/BAD ratio (Figure 4E). Repression of PAK4 resulted in reduced BAD phosphorylation (Figure 4F; online-only Data Supplement Figure IVa), which contributed to increased apoptosis in endothelial cells (Figure 3D). We also blocked miR-24 expression to derepress PAK4, which resulted in enhanced pBAD levels (Figure 4E). Knockdown of PAK4 led to reduced pBAD levels in the absence or presence of miR-24 blockade, which suggests that PAK4 is a main modulator of miR-24–mediated BAD phosphorylation in endothelial cells (online-only Data Supplement Figure VD).

To test whether the miR-24 targets GATA2, PAK4, and HMOX1 are among the main mediators of the antiangiogenic and proapoptotic action of miR-24 in endothelial cells, we reconstituted those targets in miR-24–overexpressing endothelial cells. Reconstitution of miR-24–resistant GATA2, PAK4, and HMOX1 rescued both miR-24–mediated endothelial apoptosis and miR-24–impaired tube formation capacity (Figures 4G and 4H). We thus identified a network of

Downloaded from http://circ.ahajournals.org/ by guest on August 25, 2011

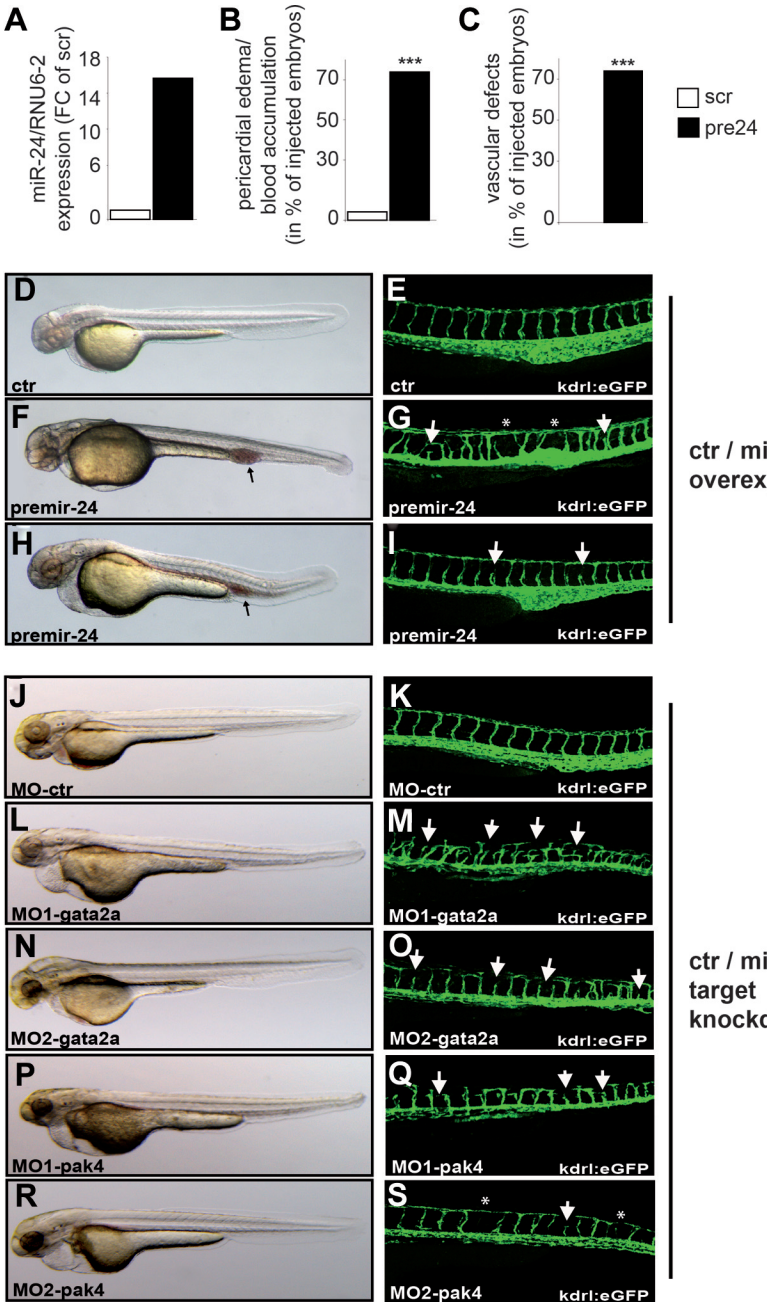

Figure 5. MiR-24 and its target genes play a role in vascularization in vivo. **A–C**, Forced expression of miR-24 in zebrafish embryos at 48 hours after fertilization (hpf) via injection of miR-24 precursors. Statistical summary (***$P<0.005$) of fish embryos that developed pericardial edema/blood accumulation defects (**B**) and vascular defects (**C**). **D–I**, Lateral views of control (scrambled sequence; **D** and **E**) and pre-miR-24–injected (**F–I**) *Tg(kdrl:eGFP)*^{s843} zebrafish embryos at 48 hpf. Embryos injected with miR-24 precursors displayed impaired and irregular vascularization patterns (asterisks and arrows in panels **G** and **I**). Pericardial edema and blood accumulation was seen after miR-24 overexpression (arrows in panels **F** and **H**). **J–S**, Lateral views of MO-*control* (**J** and **K**), MO-*gata2a* (**L–O**), and MO-*pak4* injected *Tg(kdrl:eGFP)*^{s843} (**P–S**) zebrafish embryos at 48 hpf. Knockdown of the target genes *gata2a* (**L, N**) and *pak4* (**P, R**) mimicked miR-24 overexpression, with embryos that lacked intersegmental vessels (asterisks in **G** and **S**) and displayed shortened intersegmental vessels (arrows in **G, L, M, O,** and **Q**). Furthermore, blood accumulation and pericardial edema were observed in (**M**) MO1-*gata2a*, (**O**) MO2-*gata2a,* (**Q**) MO1-*pak4*, and (**S**) MO2-*pak4* embryos, very similar to the vascularization defects seen in embryos with forced miR24 overexpression. Blood accumulation and hemorrhaging were more severe in MO-*pak4* knockdown embryos than in MO-*gata2a* injected embryos (see also online-only Data Supplement Figure VI D). ctr indicates control.

direct and indirect miR-24 targets that regulated apoptosis and angiogenic properties of endothelial cells. These important cellular characteristics may affect (neo)vascularization in vivo, especially after ischemic events.

MiR-24 Overexpression and Knockdown of miR-24 Targets Impair Zebrafish Vascular Development

To analyze miR-24 effects in vivo, we first injected miR-24 precursors into *Tg(kdrl:eGFP)*^{s843} zebrafish embryos that express GFP in the vasculature. Embryos at 48 hpf had increased miR-24 expression levels (Figure 5A), as well as abnormal vessel architecture and insufficient blood transport, which demonstrates that miR-24 activation results in a robust vascular phenotype, although we cannot exclude other cell-type–specific effects (Figures 5B through 5I). To test the involvement of the direct miR-24 targets *Gata2* and *Pak4* in this model, we used target knockdown experiments. Morpholino-based knockdown of the target gene *gata2a* (Figures 5L and 5N), as well as *pak4* (Figures 5P and 5R; online-only Data Supplement Figure VI), led to blood accumulation and pericardial edema compared with controls (Figure 5J). Furthermore, confocal images of the trunk vasculature revealed impaired vasculature formation. In MO1-*gata2a* (Figure 5M), MO2-*gata2a* (Figure 5O), MO1-*pak4* (Figure 5Q), and MO2-*pak4* (Figure 5S) embryos, we observed near-identical phenotypes to the vascularization defects seen in miR-24–overexpressing zebrafish. MiR-24–overexpression phenotypes were slightly more severe than single-gene knockdowns (eg, blood accumulation in the trunk

Downloaded from http://circ.ahajournals.org/ by guest on August 25, 2011

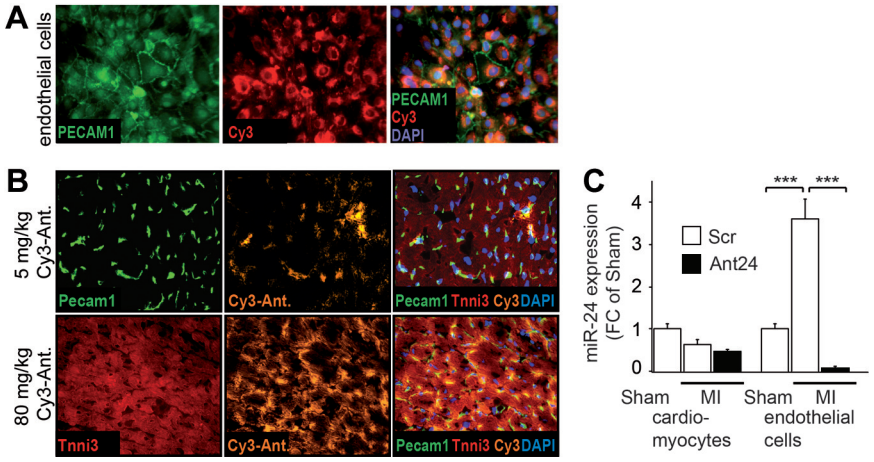

Figure 6. Low-dose antagomir-24 treatment preferably leads to miR-24 silencing in endothelial cells in vitro and in vivo. **A**, Uptake of Cy3-labeled antagomirs in human umbilical vein endothelial cells (10 μg/mL, 24 hours). **B**, Primary deposition of Cy3-labeled antagomirs (Cy3-Ant.) to platelet and endothelial cell adhesion molecule-1 (Pecam1)–positive endothelial capillaries after injection of a low dose (5 mg/kg) or homogenous cardiac uptake after treatment with 80 mg/kg (high dose). **C**, MiR-24 expression in fractionated cardiomyocytes and cardiac endothelial cells 14 days after myocardial infarction (MI). Animals were treated at day 0 and day 2 with either 5 mg/kg scrambled antagomir (Scr) or antagomir against miR-24 (Ant24). n=3 to 6 experiments/animals per group. Data are mean and SEM; ***$P<0.005$.

was more severe than cranial blood accumulation in *pak4* knockdowns; see also online-only Data Supplement Figure VI D), which is to be expected given the simultaneous effect of miR-24 on a number of genes.

Therapy With miR-24 Inhibitors Increases Vascularization and Improves Cardiac Function After MI

To further study the effects of miR-24 on vascularization in mammals, we injected chemically engineered cholesterol-conjugated single-strand RNA analogues (antagomirs) that targeted miR-24 or scrambled controls into mice. In initial experiments, we found Cy3-labeled antagomirs to be effectively taken up by endothelial cells in vitro (Figure 6A). Because we wanted to target mainly the endothelial cell fraction, we first performed titration experiments with Cy3-labeled antagomirs to achieve preferential delivery to endothelial cells. Injection of a Cy3-labeled antagomir at a low dose (5 mg/kg) mainly resulted in cellular uptake in cardiac endothelial cells, whereas injection of a high dose (80 mg/kg) led to a strong homogeneous uptake in all cardiac cells, including cardiomyocytes (Figure 6B). Consequently, we found injections of low doses of an antagomir (5 mg/kg, day 0 and day 2) against miR-24 to repress miR-24 but not unrelated miRNAs mainly in fractionated endothelial cells obtained from healthy or ischemic heart tissue (Figures 6B and 6C and data not shown).

We then tested the effects of endothelial miR-24 antagonism in a mouse model of MI. Immunohistochemical studies revealed a greater amount of apoptotic endothelial cells in the periinfarct zone (online-only Data Supplement Figure VII). In contrast, endothelial apoptosis measured by $TUNEL^+/PECAM1^+$ cells was reduced and both capillary and arteriolar density were increased in the periinfarct region after miR-24 antagonism, whereas no changes were observed in the remote myocardium (Figure 7A; online-only Data Supplement Figure VII). Improved capillary density correlated with significant smaller infarct size 14 days after MI (control 54±6% versus antagomir-24 38±3%, $P<0.05$).

MI led to an impairment of cardiac function 14 days after intervention (Figure 7B). Systolic and diastolic left ventricular diameter and lung wet weight increased after MI (Figures 7C and 7D). In contrast, immediate treatment after MI with an antagomir against miR-24 (days 0 and 2) improved cardiac function and attenuated pulmonary congestion and left ventricular dilatation (Figures 7B through 7E). Baseline data of fractional shortening and left ventricular diameters were not different between the investigated groups (data not shown). Survival of MI animals was significantly improved by miR-24 antagomir treatment (surviving animals at day 14: scrambled antagomir 43.5% versus antagomir-24 78.3%; $P=0.02$). To exclude significant off-target effects and to confirm specificity of antagomir-24, we injected an antagomir against a scrambled sequence, which did not affect miR-24 expression or infarct healing (Figures 6C and 7B through 7E). A schematic summary of our findings is presented as Figure 7F.

Discussion

In the present study, we identified miR-24 as a critical regulator of endothelial cell survival and angiogenesis. We found miR-24 to be enriched in cardiac endothelial cells and to be upregulated after ischemic injury. However, miR-24 is also expressed in other cells with different cell-specific functions, such as insulin production of pancreatic β-cells, in part via regulation of the transcriptional repressor,[49] cell cycle regulation and proliferation of leukemia cells,[50] and activation of smooth muscle cells via repression of Tribbles-like protein 1.[51] In the latter study, long-term hypoxia led to miR-24 upregulation in lung tissue and to activation of lung smooth muscle cells. Thus, inhibition of miR-24 in certain pulmonary diseases may be of future therapeutic relevance. With regard to function in other cardiac cell types, miR-24

Downloaded from http://circ.ahajournals.org/ by guest on August 25, 2011

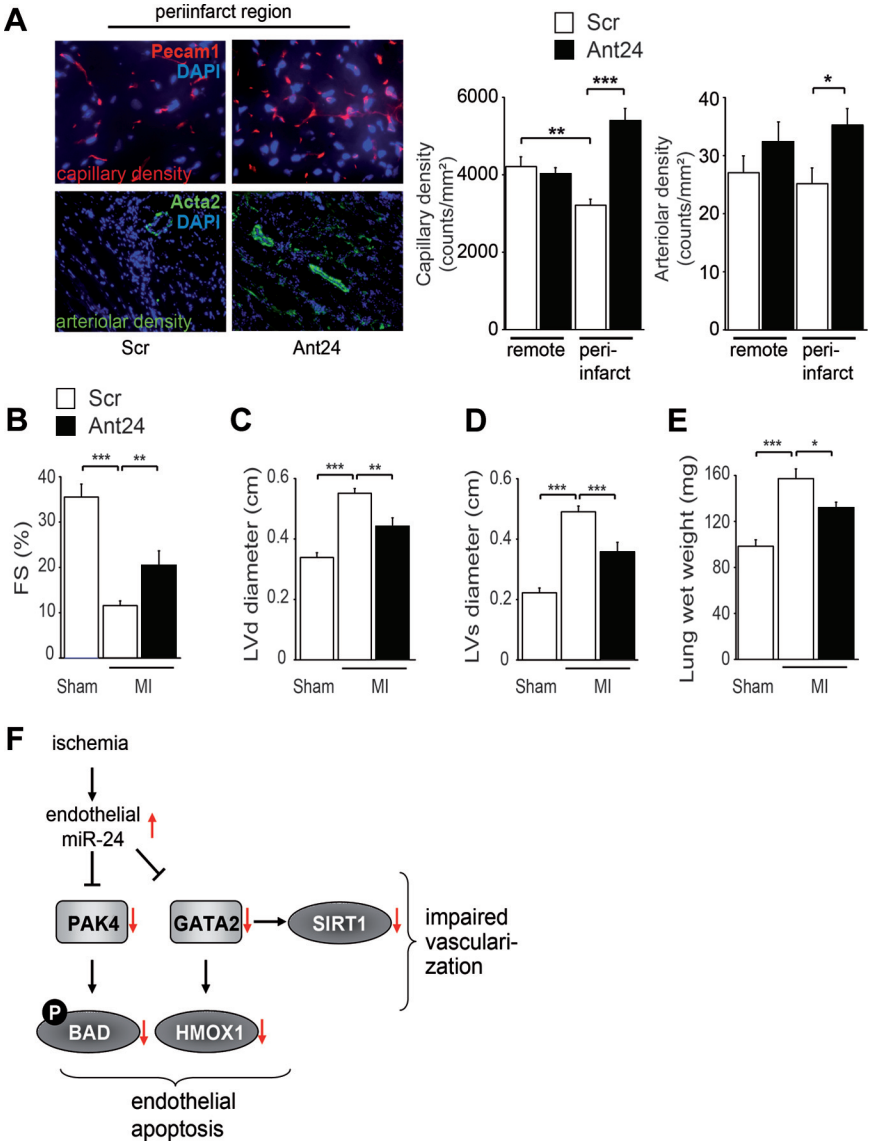

Figure 7. Antagomir-24 treatment improves vascularization and preserves cardiac function after myocardial infarction. **A**, Left, capillary (platelet and endothelial cell adhesion molecule-1 [Pecam1]) and arteriolar (Acta2) density in cardiac sections of the periinfarct region 14 days after myocardial infarction and after treatment with antagomirs against a scrambled sequence (Scr) or miR-24 (Ant24). Right, statistical summary of the number of Pecam1$^+$ capillaries and Acta2$^+$ arterioles in the remote and periinfarct area. **B**, Cardiac function as fractional shortening (FS) measured by echocardiography 14 days after sham operation or myocardial infarction (MI). Diastolic (**C**) and systolic (**D**) left ventricular diameter (LVd and LVs, respectively). **E**, Lung wet weight after sham operation or MI. **F**, Scheme of miR-24–regulated targets and downstream signaling cascades. n=6 to 9 experiments/animals per group. Data are mean and SEM; $^*P<0.05$, $^{**}P<0.01$,$^{***}P<0.005$.

overexpression has been reported to increase cardiomyocyte hypertrophy in vitro,[52] although a recent study revealed an additional role in cardiomyocyte apoptosis.[53] In that report,[53] the authors described a downregulation of miR-24 in the border zone after MI. In line with those results, we detected a downregulation of miR-24 in fractionated cardiomyocytes early after MI, whereas its expression was massively increased in cardiac endothelial cells. We used post-MI treatment with a low dose of an antagomir (2×5 mg $\cdot$ kg^{-1} $\cdot$ d^{-1}), which silenced miR-24 specifically in endothelial cells but not cardiomyocytes in the heart. Interestingly, high dosing of an antagomir (2×80 mg $\cdot$ kg^{-1} $\cdot$ d^{-1}) against miR-24 had less favorable effects on cardiac function after MI (data not shown), which suggests potential toxicity of the high-dose group or negative effects on cardiomyocyte biology, as suggested recently.[53] Future studies are therefore needed to develop improved cell-type–specific delivery systems of antagomirs. The role of miR-24 in other ischemic disease conditions and its potential therapeutic value remain to be investigated.

We used bioinformatics analyses to characterize the endothelial miR-24 targetome. So far, we have identified GATA2 (via SIRT1 and HMOX1) and PAK4 (via pBAD) as major miR-24 targets that control a complex network of apoptotic and angiogenic programs in endothelial cells (Figure 7F). However, many additional targets may be involved in the action of miR-24, especially in other disease conditions in which target availability may change. Although many other targets might be involved, target reconstitution experiments showed dominant roles of GATA2 and PAK4 for the proapoptotic and antiangiogenic effects of miR-24. The role of other potential targets important for miR-24 biological actions remains to be elucidated.

Importantly, application of low-dose antagomirs permitted silencing of miR-24 expression predominantly in endothelial cells in vivo, which resulted in reduced endothelial apoptosis, enhanced vascularization, decreased infarct size, and improved cardiac function after MI. Thus, miR-24 and its downstream targets may serve as valuable therapeutic entry points to interfere with endothelial genetic programs and

Downloaded from http://circ.ahajournals.org/ by guest on August 25, 2011

thereby improve vascularity and cardiac performance after ischemic injury.

Acknowledgments

We thank Charlotte Dienesch, Annette Horn, Michaela Kümmel, Regina Ax-Smolarski, Annette Just, Angelika Holzmann, Janet Remke, Nils Pfaff, and Marga Göbel for excellent technical assistance. We thank Kai C. Wollert and Mortimer Korf-Klingenbiel for providing the HMOX1 construct.

Sources of Funding

This work was supported in part by the German Federal Ministry of Education and Research, Integrated Research and Treatment Center (01EO0802 to T. Thum), the Integrated Center for Clinical Research (IZKF E31 to T. Thum), and the Deutsche Forschungsgemeinschaft (DFG TH903/10-1 to T. Thum). S.E. was supported by grants from the Foundation Leducq, the BMBF and the Munich Heart Alliance, Munich, Germany.

Disclosures

Drs Fiedler and Thum filed a patent application about the use of miR-24 in ischemic diseases. Dr Tuschl serves as a consultant/advisory board member for Regulus Therapeutics. The remaining authors report no conflicts of interest.

References

1. Hill JA, Olson EN. Cardiac Plasticity. *N Engl J Med*. 2008;358:1370–1380.
2. Maulik N. Angiogenic signal during cardiac repair. *Mol Cell Biochem*. 2004;264:13–23.
3. Samuel SM, Thirunavukkarasu M, Penumathsa SV, Koneru S, Zhan L, Maulik G, Sudhakaran PR, Maulik N. Thioredoxin-1 gene therapy enhances angiogenic signaling and reduces ventricular remodeling in infarcted myocardium of diabetic rats. *Circulation*. 2010;121:1244–1255.
4. Prech M, Grajek S, Marszalek A, Lesiak M, Jemielity M, Araszkiewicz A, Mularek-Kubzdela T, Cieslinski A. Chronic infarct-related artery occlusion is associated with a reduction in capillary density: effects on infarct healing. *Eur J Heart Fail*. 2006;8:373–380.
5. Ambros V. The functions of animal microRNAs. *Nature*. 2004;431:350–355.
6. Thum T, Gross C, Fiedler J, Fischer T, Kissler S, Bussen M, Galuppo P, Just S, Rottbauer W, Frantz S, Castoldi M, Soutschek J, Koteliansky V, Rosenwald A, Basson MA, Licht JD, Pena JT, Rouhanifard SH, Muckenthaler MU, Tuschl T, Martin GR, Bauersachs J, Engelhardt S. MicroRNA-21 contributes to myocardial disease by stimulating MAP kinase signalling in fibroblasts. *Nature*. 2008;456:980–984.
7. Bonauer A, Carmona G, Iwasaki M, Mione M, Koyanagi M, Fischer A, Burchfield J, Fox H, Doebele C, Ohtani K, Chavakis E, Potente M, Tjwa M, Urbich C, Zeiher AM, Dimmeler S. MicroRNA-92a controls angiogenesis and functional recovery of ischemic tissues in mice. *Science*. 2009;324:1710–1713.
8. Care A, Catalucci D, Felicetti F, Bonci D, Addario A, Gallo P, Bang ML, Segnalini P, Gu Y, Dalton ND, Elia L, Latronico MVG, Hoydal M, Autore C, Russo MA, Dorn GW, Ellingsen O, Ruiz-Lozano P, Peterson KL, Croce CM, Peschle C, Condorelli G. MicroRNA-133 controls cardiac hypertrophy. *Nat Med*. 2007;13:613–618.
9. Ren XP, Wu J, Wang X, Sartor MA, Qian J, Jones K, Nicolaou P, Pritchard TJ, Fan GC. MicroRNA-320 is involved in the regulation of cardiac ischemia/reperfusion injury by targeting heat-shock protein 20. *Circulation*. 2009;119:2357–2366.
10. van Rooij E, Sutherland LB, Thatcher JE, DiMaio JM, Naseem RH, Marshall WS, Hill JA, Olson EN. Dysregulation of microRNAs after myocardial infarction reveals a role of miR-29 in cardiac fibrosis. *Proc Natl Acad Sci U S A*. 2008;105:13027–13032.
11. van Rooij E, Sutherland LB, Qi X, Richardson JA, Hill J, Olson EN. Control of stress-dependent cardiac growth and gene expression by a MicroRNA. *Science*. 2007;316:575–579.
12. Small EM, Olson EN. Pervasive roles of microRNAs in cardiovascular biology. *Nature*. 2011;469:336–342.
13. Kuehbacher A, Urbich C, Zeiher AM, Dimmeler S. Role of Dicer and Drosha for endothelial MicroRNA expression and angiogenesis. *Circ Res*. 2007;101:59–68.
14. Suarez Y, Fernandez-Hernando C, Pober JS, Sessa WC. Dicer dependent MicroRNAs regulate gene expression and functions in human endothelial cells. *Circ Res*. 2007;100:1164–1173.
15. Suarez Y, Fernandez-Hernando C, Yu J, Gerber SA, Harrison KD, Pober JS, Iruela-Arispe ML, Merkenschlager M, Sessa WC. Dicer-dependent endothelial microRNAs are necessary for postnatal angiogenesis. *Proc Natl Acad Sci U S A*. 2008;105:14082–14087.
16. Wang S, Aurora AB, Johnson BA, Qi X, McAnally J, Hill JA, Richardson JA, Bassel-Duby R, Olson EN. The endothelial-specific microRNA miR-126 governs vascular integrity and angiogenesis. *Dev Cell*. 2008;15:261–271.
17. Poliseno L, Tuccoli A, Mariani L, Evangelista M, Citti L, Woods K, Mercatanti A, Hammond S, Rainaldi G. MicroRNAs modulate the angiogenic properties of HUVECs. *Blood*. 2006;108:3068–3071.
18. Kulshreshtha R, Ferracin M, Wojcik SE, Garzon R, Alder H, Agosto-Perez FJ, Davuluri R, Liu CG, Croce CM, Negrini M, Calin GA, Ivan M. A MicroRNA signature of hypoxia. *Mol Cell Biol*. 2007;27:1859–1867.
19. Landgraf P, Rusu M, Sheridan R, Sewer A, Iovino N, Aravin A, Pfeffer S, Rice A, Kamphorst AO, Landthaler M, Lin C, Socci ND, Hermida L, Fulci V, Chiaretti S, Foa R, Schliwka J, Fuchs U, Novosel A, Muller RU, Schermer B, Bissels U, Inman J, Phan Q, Chien M, Weir DB, Choksi R, De Vita G, Frezzetti D, Trompeter HI, Hornung V, Teng G, Hartmann G, Palkovits M, Di Lauro R, Wernet P, Macino G, Rogler CE, Nagle JW, Ju J, Papavasiliou FN, Benzing T, Lichter P, Tam W, Brownstein MJ, Bosio A, Borkhardt A, Russo JJ, Sander C, Zavolan M, Tuschl T. A mammalian microRNA expression atlas based on small RNA library sequencing. *Cell*. 2007;129:1401–1414.
20. Zhou Q, Gallagher R, Ufret-Vincenty R, Li X, Olson EN, Wang S. Regulation of angiogenesis and choroidal neovascularization by members of microRNA-23~27~24 clusters. *Proc Natl Acad Sci U S A*. 2011;108:8287–8292.
21. Thum T, Galuppo P, Wolf C, Fiedler J, Kneitz S, van Laake LW, Doevendans PA, Mummery CL, Borlak J, Haverich A, Gross C, Engelhardt S, Ertl G, Bauersachs J. MicroRNAs in the human heart: a clue to fetal gene reprogramming in heart failure. *Circulation*. 2007;116:258–267.
22. Weinmann AS, Bartley SM, Zhang T, Zhang MQ, Farnham PJ. Use of chromatin immunoprecipitation to clone novel E2F target promoters. *Mol Cell Biol*. 2001;21:6820–6832.
23. Messeguer X, Escudero R, Farre D, Nunez O, Martinez J, Alba MM. PROMO: detection of known transcription regulatory elements using species-tailored searches. *Bioinformatics*. 2002;18:333–334.
24. Farre D, Roset R, Huerta M, Adsuara JE, Rosello L, Alba MM, Messeguer X. Identification of patterns in biological sequences at the ALGGEN server: PROMO and MALGEN. *Nucleic Acids Res*. 2003;31:3651–3653.
25. Walker MB, Miller CT, Swartz ME, Eberhart JK, Kimmel CB. Phospholipase C, beta 3 is required for endothelin1 regulation of pharyngeal arch patterning in zebrafish. *Dev Biol*. 2007;304:194–207.
26. Galloway JL, Wingert RA, Thisse C, Thisse B, Zon LI. Loss of gata1 but not gata2 converts erythropoiesis to myelopoiesis in zebrafish embryos. *Dev Cell*. 2005;8:109–116.
27. Galloway JL, Wingert RA, Thisse C, Thisse B, Zon LI. Combinatorial regulation of novel erythroid gene expression in zebrafish. *Exp Hematol*. 2008;36:424–432.
28. Frantz S, Hu K, Bayer B, Gerondakis S, Strotmann J, Adamek A, Ertl G, Bauersachs J. Absence of NF-κB subunit p50 improves heart failure after myocardial infarction. *FASEB J*. 2006;20:1918–1920.
29. Merkle S, Frantz S, Schon MP, Bauersachs J, Buitrago M, Frost RJA, Schmitteckert EM, Lohse MJ, Engelhardt S. A role for caspase-1 in heart failure. *Circ Res*. 2007;100:645–653.
30. Mammoto A, Connor KM, Mammoto T, Yung CW, Huh D, Aderman CM, Mostoslavsky G, Smith LEH, Ingber DE. A mechanosensitive transcriptional mechanism that controls angiogenesis. *Nature*. 2009;457:1103–1108.
31. Koh W, Mahan RD, Davis GE. Cdc42- and Rac1-mediated endothelial lumen formation requires Pak2, Pak4 and Par3, and PKC-dependent signaling. *J Cell Sci*. 2008;121:989–1001.
32. Eerola I, Boon LM, Mulliken JB, Burrows PE, Dompmartin A, Watanabe S, Vanwijck R, Vikkula M. Capillary malformation-arteriovenous malformation, a new clinical and genetic disorder caused by RASA1 mutations. *Am J Hum Genet*. 2003;73:1240–1249.

Downloaded from http://circ.ahajournals.org/ by guest on August 25, 2011

33. Bryant P, Zheng Q, Pumiglia K. Focal adhesion kinase controls cellular levels of p27/Kip1 and p21/Cip1 through Skp2-dependent and-independent mechanisms. *Mol Cell Biol*. 2006;26:4201–4213.
34. Ernkvist M, Persson NL, Audebert S, Lecine P, Sinha I, Liu M, Schlueter M, Horowitz A, Aase K, Weide T, Borg JP, Majumdar A, Holmgren L. The Amot/Patj/Syx signaling complex spatially controls RhoA GTPase activity in migrating endothelial cells. *Blood*. 2009;113:244–253.
35. Economopoulou M, Langer HF, Celeste A, Orlova VV, Choi EY, Ma M, Vassilopoulos A, Callen E, Deng C, Bassing CH, Boehm M, Nussenzweig A, Chavakis T. Histone H2AX is integral to hypoxia-driven neovascularization. *Nat Med*. 2009;15:553–558.
36. Carmona G, Gottig S, Orlandi A, Scheele J, Bauerle T, Jugold M, Kiessling F, Henschler R, Zeiher AM, Dimmeler S, Chavakis E. Role of the small GTPase Rap1 for integrin activity regulation in endothelial cells and angiogenesis. *Blood*. 2009;113:488–497.
37. D'Arcangelo D, Ambrosino V, Giannuzzo M, Gaetano C, Capogrossi MC. Axl receptor activation mediates laminar shear stress anti-apoptotic effects in human endothelial cells. *Cardiovasc Res*. 2006;71:754–763.
38. Michaud MD, Robitaille GA, Gratton JP, Richard DE. Sphingosine-1-phosphate: a novel nonhypoxic activator of hypoxia-inducible factor-1 in vascular cells. *Arterioscler Thromb Vasc Biol*. 2009;29:902–908.
39. Sakurai A, Fukuhara S, Yamagishi A, Sako K, Kamioka Y, Masuda M, Nakaoka Y, Mochizuki N. MAGI-1 is required for Rap1 activation upon cell-cell contact and for enhancement of vascular endothelial cadherin-mediated cell adhesion. *Mol Biol Cell*. 2006;17:966–976.
40. Provencal M, Michaud M, Beaulieu E, Ratel D, Rivard GE, Gingras D, Beliveau R. Tissue factor pathway inhibitor (TFPI) interferes with endothelial cell migration by inhibition of both the Erk pathway and focal adhesion proteins. *Thromb Haemost*. 2008;99:576–585.
41. Lee HJ, Cho CH, Hwang SJ, Choi HH, Kim KT, Ahn SY, Kim JH, Oh JL, Lee GM, Koh GY. Biological characterization of angiopoietin-3 and angiopoietin-4. *FASEB J*. 2004;18:1200–1208.
42. Scharpfenecker M, van Dinther M, Liu Z, van Bezooijen RL, Zhao Q, Pukac L, Lowik CWGM, Ten Dijke P. BMP-9 signals via ALK1 and inhibits bFGF-induced endothelial cell proliferation and VEGF-stimulated angiogenesis. *J Cell Sci*. 2007;120:964–972.
43. Thum T, Haverich A, Borlak J. Cellular dedifferentiation of endothelium is linked to activation and silencing of certain nuclear transcription factors: implications for endothelial dysfunction and vascular biology. *FASEB J*. 2000;14:740–751.
44. Tian Y, Lei L, Cammarano M, Nekrasova T, Minden A. Essential role for the Pak4 protein kinase in extraembryonic tissue development and vessel formation. *Mech Dev*. 2009;126:710–720.
45. Potente M, Ghaeni L, Baldessari D, Mostoslavsky R, Rossig L, Dequiedt F, Haendeler J, Mione M, Dejana E, Alt FW, Zeiher AM, Dimmeler S. SIRT1 controls endothelial angiogenic functions during vascular growth. *Genes Dev*. 2007;21:2644–2658.
46. Lin HH, Chen YH, Chang PF, Lee YT, Yet SF, Chau LY. Heme oxygenase-1 promotes neovascularization in ischemic heart by coinduction of VEGF and SDF-1. *J Mol Cell Cardiol*. 2008;45:44–55.
47. Lal A, Pan Y, Navarro F, Dykxhoorn DM, Moreau L, Meire E, Bentwich Z, Lieberman J, Chowdhury D. miR-24-mediated downregulation of H2AX suppresses DNA repair in terminally differentiated blood cells. *Nat Struct Mol Biol*. 2009;16:492–498.
48. Gnesutta N, Qu J, Minden A. The serine/threonine kinase PAK4 prevents caspase activation and protects cells from apoptosis. *J Biol Chem*. 2001;276:14414–14419.
49. Melkman-Zehavi T, Oren R, Kredo-Russo S, Shapira T, Mandelbaum AD, Rivkin N, Nir T, Lennox KA, Behlke MA, Dor Y, Hornstein E. miRNAs control insulin content in pancreatic beta-cells via downregulation of transcriptional repressors. *EMBO J*. 2011;30:835–845.
50. Lal A, Navarro F, Maher CA, Maliszewski LE, Yan N, O'Day E, Chowdhury D, Dykxhoorn DM, Tsai P, Hofmann O, Becker KG, Gorospe M, Hide W, Lieberman J. miR-24 inhibits cell proliferation by targeting E2F2, MYC, and other cell-cycle genes via binding to "seedless" 3′UTR microRNA recognition elements. *Mol Cell*. 2009;35:610–625.
51. Chan MC, Hilyard AC, Wu C, Davis BN, Hill NS, Lal A, Lieberman J, Lagna G, Hata A. Molecular basis for antagonism between PDGF and the TGFbeta family of signalling pathways by control of miR-24 expression. *EMBO J*. 2010;29:559–573.
52. van Rooij E, Sutherland LB, Liu N, Williams AH, McAnally J, Gerard RD, Richardson JA, Olson EN. A signature pattern of stress-responsive microRNAs that can evoke cardiac hypertrophy and heart failure. *Proc Natl Acad Sci U S A*. 2006;103:18255–18260.
53. Qian L, Van Laake LW, Huang Y, Liu S, Wendland MF, Srivastava D. miR-24 inhibits apoptosis and represses Bim in mouse cardiomyocytes. *J Exp Med*. 2011;208:549–560.

CLINICAL PERSPECTIVE

Ischemic heart disease is the leading cause of death worldwide, often presenting as acute myocardial infarction. Myocardial infarction frequently progresses to the development of heart failure. Insufficient myocardial vascularization prevents optimal blood support for cardiomyocyte survival, although the underlying mechanisms of cardiac vascularization are not well understood. MicroRNAs are small RNA molecules regulating approximately half of the genome and recently have emerged as powerful therapeutic targets for various heart diseases. We identified miRNA-24 (miR-24) as being activated in cardiac endothelial cells after myocardial infarction, leading to endothelial cell apoptosis and abolishment of capillary network formation. These effects are mediated through targeting of the endothelium-enriched transcription factor GATA2, the p21-activated kinase PAK4, and the respective downstream signaling cascades. Blocking of endothelial miR-24 in a mouse model of myocardial infarction limits myocardial infarct size by preventing endothelial apoptosis and enhancing vascularity, which leads to preserved cardiac function and survival. Thus, miR-24 acts as a critical regulator of cardiac vascularization and is suitable for therapeutic intervention in the setting of ischemic heart disease. Our findings may lead to clinical applications, whereby miRNA modulators are used systemically or locally to improve vascularization in patients after myocardial infarction.

Downloaded from http://circ.ahajournals.org/ by guest on August 25, 2011

SUPPLEMENTAL MATERIAL

Expanded Methods and Results

Cultivation of cardiovascular cells. Human umbilical vein endothelial cells (HUVECs) were cultured in EGM2 media supplemented with 10% (v/v) fetal calf serum (FCS) and supplements (all reagents from Cambrex Lonza, UK). Cells were grown in a humidified atmosphere at 5% CO_2 and 37°C.

Fractionation of cardiac cell types from heart tissue. The thorax of mice was opened and the aorta was cannulated. After washing with 37°C PBS, the heart together with the cannula was removed and perfused with a collagenase solution for 5 min (Joklik MEM medium supplemented with 10 mM butanedione monoxime, 20 µM calcium chloride, 1mg/ml collagenase II) as described [1]. Then the heart was placed in 37°C pre-warmed collagenase solution for further 25 min and was subsequently divided in infarct and remote areas, minced and filtered through a nylon mesh (200 µm pore size). Then, cardiomyocytes and cardiac fibroblasts were separated by a sedimentation step as described [2]. Within the non-cardiomyocyte cell fraction retained in the supernatant an incubation step with CD146-antibodies coupled to microbeads was performed and subjected to magnetic affinity cell sorting according to the manufacturers' recommendations (Mouse CD146 microbead endothelial isolation kit, Miltenyi Biotec, Germany).

Apoptosis protein array. Apoptosis array data were generated by applying a human apoptosis array kit (ARY009, R&D, USA). 200 µg protein from a pool of three samples were incubated with antibody-coated membranes following manufacturers´ instructions. Various regulated proteins were then validated by Western blotting.

Downloaded from http://circ.ahajournals.org/ by guest on August 25, 2011

Detection of reactive oxygen species (ROS). The redox-sensitive, cell-permeable fluorophore dihydroethidium (DHE) becomes oxidized in the presence of O_2^- to yield fluorescent ethidium. Thus, dye oxidation is an indirect measure of the presence of reactive oxygen intermediates [3]. MiRNA-transfected HUVECs were incubated with DHE (2.5 µM) for 30 min. After washing, HUVECs were immediately analyzed with FACS (FACS Calibur, BD Bioscience).

MircoRNA target prediction. The microRNA databases and target prediction tools miRBase (http://microrna.sanger.ac.uk/), PicTar (http://pictar.mdc-berlin.de/) and TargetScan (http://www.targetscan.org/index.html) were used to identify potential microRNA targets. Specifically, we searched for targets with known expression in cardiovascular tissue and endothelial cells. We focused on targets predicted by at least two prediction data bases and containing a miR-24-8mer seed match in the respective 3'UTR region.

***In situ* hybridization.**

We combined in situ hybridization of miR-24 with endothelial and smooth muscle cell marker stainings. Mouse heart cryosections (10 µm) were dried at room temperature and fixed with 4% PFA for 10 min. at room temperature and washed two times with DEPC-PBS for 3 min. To increase tissue permeability and reduce unspecific background, the sections were treated with proteinase K (end concentration 5 µg/ ml) for 15 min at 37°C and then were washed two times for 3 minutes with DEPC-PBS. The sections were acetylated 15 minutes at room temperature using acetic anhydride dissolved in DEPC- water, 6N HCl and Triethanolamine and subsequently washed two times with DEPC-PBS for 3 min. Pre-hybridisation was performed 1 hour at 60°C in pre-hybridization buffer containing 50% formamide, 5x SSC, 0.5 mg/ml yeast tRNA, 1x Denhardt's solution and 9.2 mM citric acid. Subsequently, sections were hybridized with 2.5 pmol of miR-24- specific probe labelled with fluorescein at 5' end (# 18121-04, Exiqon) or with fluorescein labelled scrambled miR- probe (#99004-04, Exiqon) diluted in pre-hybridization buffer, overnight at 60°C. The described RNA melting

Downloaded from http://circ.ahajournals.org/ by guest on August 25, 2011

temperature of the miR-24 and scrambled control were approximately similar (±3 °C). Next day, the sections were washed three times with 0.1x SSC at 65°C and, finally, one time with 2x SSC for 5 min, permeabilized for immunostaining with 0.1% Triton X-100 and washed 2 times with PBS. Unspecific background was blocked with 5% donkey serum diluted in PBS 30 min. at room temperature. Endothelial cells were stained with rat anti- CD31 antibody (# MCA 2388, AbD Serotec) at 1:50 dilution for 2 hours at room temperature and sections were washed several times with PBS. Smooth muscle cells were stained with rabbit anti-alpha smooth muscle actin antibody (Acta2; ab5694, Abcam) at 1:50 dilution overnight at 4°C. Then, sections were incubated with donkey anti-rat- AlexaFluor594 antibody (#21209, Invitrogen; dilution 1:500; to detect Pecam1) or with donkey anti-rabbit- AlexaFluor594 antibody (#21207, Invitrogen dilution 1:500; to detect Acta2) together with DAPI (1: 1000), for 30 min at room temperature, washed several times with PBS and mounted the sections using VectaShield Hard Set (#H-1400, Vector laboratories) mounting medium.

Immunofluorescence. Frozen heart sections were acetone-fixed, washed and blocked with 5% (v/v) donkey sera or MOM Mouse IgGs (for RASA1 stain) before addition of appropriate Alexa-conjugated secondary antibodies (Invitrogen). Slides were mounted in VECTASHIELD/DAPI (Linaris, Germany). Details about used antibodies are shown in **Supplemental Table 3**.

Chromatin immunoprecipitation. Chromatin immunoprecipitation (ChIP) was used to detect protein-DNA interactions. First, protein G sepharose beads were blocked o/n at 4°C. HUVECs from confluent T75 flasks were first cross-linked and harvested. The pellet was lysed and sonified to yield DNA fragments from 100-1000 bp in length. Afterwards, samples were centrifuged at maximum speed to yield cleared lysates. Aliquots were separately taken to measure sonification efficiency by agarose gel analysis. To reduce non-specific background, cleared lysates were pre-cleared on blocked Protein G Sepharose beads (GE Healthcare) twice. Samples were subjected to either immunoprecipitation with 5 µg GATA2

Downloaded from http://circ.ahajournals.org/ by guest on August 25, 2011

antibody (Santa Cruz Biotechnology, sc-267X) or control mouse IgGs (Santa Cruz Biotechnology, sc-2025) o/n at 4 °C. To block non-specific background BSA and herring sperm DNA were added. One sample with cell lysis and IP dilution buffer was used as mock control. The next day GATA2/DNA cross-links were collected by incubation with Protein G beads. Beads were washed twice with dialysis buffer and four times with IP wash buffer. Finally, beads were washed twice with TE-buffer. Antibody-GATA2/DNA complexes were eluted from the beads by adding 150 µl IP elution buffer and heating at 65°C. The elution step was repeated and combined eluates were reverse cross-linked. Samples were subjected to RNA and protein degradation. Afterwards, DNA was isolated and purified with Qiagen PCR purification kit (Qiagen).

For ChIP primer-design we first identified 2000-2500 bp upstream promoter region of candidate target genes by Ensembl Genome Browser (http://www.ensembl.org/index.html). Then we screened the promoter region for potential GATA2 binding sites by the use of ALLGEN-Promo and selected appropriate primer pairs that amplify potential GATA2 binding sites. Subsequent PCR analysis of chipped DNA fragments was done by mixing 2.5 µl sample, 2.5 µl 4 µM appropriate primer pairs, 10 µl HotStarTaq Mix (Qiagen) and applying the following protocol: 94°C 10 min, [94°C 1 min, 57°C 30 sec, 72°C 1 min]x33, 72°C 10 min, 4°C hold. Used oligonucleotide primer sequences are given in **Supplemental Table 4.**

Antagomir injection. Antagomirs were designed and provided by Regulus Therapeutics (USA) and as described [4]. Sequences were: Antagomir-24: 5'-CTGTTCCTGCTGAACTGAGCCA-chol-3' and scrambled Antagomir: 5'-ACAAACACCAUUGUCACACUCCA-chol-3'. Antagomirs were diluted in nuclease-free water and 100 µl at concentrations of 5 mg/kg and 80 mg/kg were applied to mice via retroorbital injection.

Determination of apoptotic endothelial cells and cardiomyocytes in vivo. Apoptosis was quantified at 14 days after MI by terminal deoxynucleotidyltransferase (TdT)-mediated dUTP

Downloaded from http://circ.ahajournals.org/ by guest on August 25, 2011

nick-end labeling (TUNEL) technique (in situ cell death detection kit Fluorescein, Roche, Germany) and combined cell-type specific stainings of either endothelial cells (Pecam1) or cardiomyoctyes (Tnni3). Following treatment of slides with proteinase K (20µg/ml, 30min at 37°C), TUNEL assay was performed as described by the manufacturer. Sections were additionally stained with DAPI to recognize nuclei. At least ten high power fields (400x) from the peri-infarct zone were analysed.

Myocardial infarction. Male Mice (C57BL/6, 8-10 weeks) underwent coronary artery ligation for the production of myocardial infarction (MI). Successful generation of MI after occlusion of the left ascending artery was monitored by parallel electrocardiogram (ECG; ST-elevation) measurements and impaired wall motion by echocardiography. Only mice with significant ST-elevation in the ECG analysis and impaired wall motion by echocardiography were included in the study. Briefly, mice were anesthetized, placed on a heating pad, intubated and ventilated with a mixture of oxygen and isoflurane. After left lateral thoracotomy and exposure of the heart by retractors, the left anterior descending coronary artery (LAD) was permanently ligated. Successful production of MI was checked by measurements of ST-elevation in electrocardiograms as well as impaired left ventricular wall motion by echocardiography. Animals that did not show ST-elevation and impaired left ventricular wall motion after myocardial infarction were excluded from further studies. Fourteen days after MI, additional echocardiography measurements were performed and finally hearts were excised and cut into transverse sections. From the middle ring, sections were cut and stained with appropriate antibodies (see above). Cardiac dimensions and function were analyzed by pulse–wave Doppler echocardiography.

Determination of infarct size. This was done essentially as described previously [5]. From cardiac rings sections were stained with picrosirius red and infarct size was determined by planimetric measurement using a microscope and calculated by dividing the sum of

Downloaded from http://circ.ahajournals.org/ by guest on August 25, 2011

endocardial and epicardial circumferences of infarct areas by the sum of the total endocardial and epicardial circumferences.

Downloaded from http://circ.ahajournals.org/ by guest on August 25, 2011

Additional Figures

Figure legends

Supplemental Figure 1. MiR-24 inhibits endothelial tube formation independently from its pro-apoptotic activity but has no effects on number and function of endothelial progenitor cells. Endothelial tube formation 72 h after transfection of scrambled miRNAs (scr-miR, 100 nM) or miR-24 precursors (pre-miR-24, 100 nM) in the presence or absence of a pan-caspase inhibitor (Caspase 3 inhibitor I, 100 µm, 72 h). **P,0.01. n=3-5 per group.

Supplemental Figure 2. Regulation and functional importance of further miR-24 targets RASA1 and H2AFX in endothelial cells. (**a**) Western Blots of RASA1 and H2AFX 72 h after transfection of scrambled (scr-miR) or miR-24 precursors (pre-24). (**b**) Activities of luciferase reporter constructs comprising the 3'UTR region of *RASA1* and *H2AFX* mRNA relative to beta-Gal control plasmids after transfection of synthetic miRNAs. (**c**) Western blots of RASA1 and H2AFX 48 h after transfection of specific siRNAs against RASA1, H2AFX or appropriate control siRNAs (si-scr). TBP=TATA box binding protein (nuclear housekeeping protein). (**d**) Relative changes in apoptosis (Annexin V-assay) and changes in tube formation (**e**) 48h after transfection of specific siRNAs against RASA1, H2AFX or appropriate scrambled siRNAs. n=3-4 experiments per group. Data are mean and s.e.m.; *P,0.05, ***P,0.005.

Supplemental Figure 3. Cardiac endothelial expression of miR-24 targets. (**a**) Localization of endothelial protein Pecam1 and the miR-24 targets Gata2, Pak4 and Rasa1 in sections of mouse hearts. Nuclei were counterstained with 4',6-diamidin-2'-phenylindol-dihydrochlorid (DAPI). White arrows indicate perinuclear region of PAK4 expression in cardiac endothelial cells. (**b**) Protein expression of *miR-24* targets in fractionated cardiomyoctyes and cardiac endothelial cells. n=3-4 experiments per group.

Supplemental Figure 4. MiR-24 target modulation in endothelial cells. (**a**) Expression of GATA2 and PAK4 48h after transfection of specific siRNAs against GATA2 or PAK4 or scrambled controls (si-scr). *Right*, Statistical summary. (**b**) Gata2 expression three days after transfection of a murine GFP-Gata2 construct or a YFP-labeled control construct to human umbilical vein endothelial cells. Note, cytoplasmic localisation of the control construct and nuclear expression of the GFP-Gata2 construct. (**c**) Western blots of SIRT1 after up- or downregulation of GATA2 in HUVECs. (**d**) SIRT1 expression after transfection of increasing doses (m.o.i.) of the adenoviral GATA2 construct to endothelial cells. n=3-4 experiments per group. Data are mean and s.e.m.; *P,0.05; ***P,0.005.

Supplemental Figure 5. MiR-24 regulates HMOX1 expression via GATA2 and Bad phosphorylation via PAK4 in endothelial cells. (**a**) HMOX1 expression is regulated by miR-24 in endothelial cells.(**b**) GATA2 and HMOX1 expression in endothelial cells after miR-24 inhibition and/or GATA2 silencing. (**c**) FACS-based analysis of ROS formation 72 h after transfection of synthetic miR-24 precursors (pre-24) or scrambled controls (scr) to HUVECs. (**d**) BAD phosphorylation in endothelial cells after *miR-24* inhibition and/or PAK4 silencing. n=3-6 experiments per group. Data are mean and s.e.m.; *P,0.05, **P,0.01, ***P,0.005.

Supplemental Figure 6. Knockdown strategy for *pak4*. (**a,b**) Lateral view of 24 hpf zebrafish embryos injected with (**a, a'**) cRNA containing Pak4-morpholino target site in front of a cassette encoding GFP and 4 ng of control morpholino or (**b, b'**) cRNA containing Pak4-morpholino target site in front of a cassette encoding GFP and 4 ng of MO1-*pak4.* (**a'**) Whereas the control embryos displayed GFP expression, (**b**) GFP expression was suppressed by silencing of the Pak4-target site after injection of MO1-*pak4* morpholino. (**c**) The splice site morpholino MO2-*pak4* was directed against the exon 5, intron 5 boundary of

Downloaded from http://circ.ahajournals.org/ by guest on August 25, 2011

pak4 which consists of 10 exons. Arrows depict the location of the two primers which were utilized in the RT-PCR analysis. RT-PCR analysis of total RNA isolated of MO2-*pak4* and control morpholino injected embryos at 24 hpf revealed a significant decrease of correctly spliced *pak4* transcripts in MO2-*pak4* morphants in contrast to the control. RT-PCR analysis of ß-actin served as loading control. (**d**) A representative *pak4*-MO2 injected embryo at 48hpf displaying blood accumulation and hemorrhaging (arrows) in the trunk and head region. In this particular experiment, 110 embryos were scored and 74 displayed blood retention and compromised circulation. 11 embryos had hemorrhages.

Supplemental Figure 7. Prevention of endothelial apoptosis in vivo by antagomir-24 treatment. Apoptotic endothelial cells ($TUNEL^+/Pecam1^+$ cells) within the periinfarct region 14 d after myocardial infarction (MI) and treatment with scrambled antagomirs (Scr) or antagomir-24 (Ant24). *Bottom*, Statistical summary. n=6-8 experiments per group. Data are mean and s.e.m.; **P,0.01.

Downloaded from http://circ.ahajournals.org/ by guest on August 25, 2011

Additional Tables

Supplemental Table 1: TaqMan miRNA detection assays

miRNA	Reference
miR-24	Assay ID 000402, Applied Biosystems, USA
RNU6-2	Assay ID 001093, Applied Biosystems, USA

Supplemental Table 2: Used siRNAs and miRNAs

siRNAs

siRNA	Reference
GATA2	sc-37228, Santa Cruz Biotechnology, USA
PAK4	sc-39060, Santa Cruz Biotechnology, USA
H2AFX	sc-62464, Santa Cruz Biotechnology, USA
RASA1	sc-29467, Santa Cruz Biotechnology, USA
Drosha	[6]
scrambled siRNA control-A	sc-37007, Santa Cruz Biotechnology, USA

miRNAs

miRNA	Reference
miR-24	PM10737, Applied Biosystems, USA
anti-miR-24	AM10737, Applied Biosystems, USA
miR-22	PM11752, Applied Biosystems, USA
miR-210	PM10516, Applied Biosystems, USA
pre-miR. precursor molecules-negative control #2	PM17111, Applied Biosystems, USA

Supplemental Table 3: Antibodies applied in this work for Western blotting and immunofluorescence

Antibody	Reference	Immunization
GAPDH	ab8245, Abcam, USA	mouse
GATA2	arp31855, Aviva Systems Biology, USA	rabbit
GFP	ab1218, Abcam, USA	mouse
HMOX1	AF3776, R&D Systems, USA	goat
PAK4	ab19007, Abcam, USA	rabbit
BAD	ab28840, Abcam, USA	rabbit
RASA1	ab2922, Abcam, USA	mouse
SIRT1	ab32441, Abcam, USA	rabbit
H2AFX	ab11175, Abcam, USA	rabbit
TBP	ab818, Abcam, USA	mouse
PECAM1	#2388, AbD Serotec, Germany	rat
TNNI3	sc-15368, Santa Cruz Biotechnology, USA	rabbit
ACTN2	ab15734, Abcam, USA	rabbit

Downloaded from http://circ.ahajournals.org/ by guest on August 25, 2011

Supplemental Table 4: Primers used for ChIP-PCR

Promoter region	primer (forward, reverse)	Product size [bp]
BMP and activin membrane-bound inhibitor (BAMBI)	forward: 5´-tctcaggttttggagggaga-3´ reverse: 5´-ggccgagactgacactcaat-3´	259
Endothelial cell specific molecule 1 (ESM1)	forward: 5´- caagtgatatgccagggtca -3´ reverse: 5´- tggttgttttgcatgaggac -3´	136
Heme oxygenase 1 (HMOX1)	forward: 5´- catcaccagacccagacaga-3´ reverse: 5´- aaggccgactttaagggaag-3´	133
Netrin 4 (NTN4)	forward: 5´-gagccagttattcagcaaagaaa-3´ reverse: 5´-atgcagaggccatgctaatc-3´	180
Sirtuin 1 (SIRT1)	forward: 5´-ggagtcacagtgtgccagaa-3´ reverse: 5´-ccttcctttctagcgtgagc-3´	201

Supplemental Table 5: Morpholino sequences for target knockdown studies in zebrafish

name	sequence
MO1-gata2a	5' - CATCTACTCACCAGTCTGCGCTTTG - 3'
MO2-gata2a	5' - AATGAATCCTACCGTGCGCTTGTCC – 3´
MO1-pak4	5‘- GCTTTTTCTTGCTGAACATGGC - 3‘
MO2-pak4	5‘ – TTCCTGTGTGTTGCACCAACCTCAT – 3‘

Downloaded from http://circ.ahajournals.org/ by guest on August 25, 2011

References (to Expanded Methods)

1. Thum T, Borlak J. Reprogramming of gene expression in cultured cardiomyocytes and in explanted hearts by the myosin ATPase inhibitor butanedione monoxime. Transplantation. 2001; 71: 543-552.

2. Thum T, Gross C, Fiedler J, Fischer T, Kissler S, Bussen M, Galuppo P, Just S, Rottbauer W, Frantz S, Castoldi M, Soutschek J, Koteliansky V, Rosenwald A, Basson MA, Licht JD, Pena JT, Rouhanifard SH, Muckenthaler MU, Tuschl T, Martin GR, Bauersachs J, Engelhardt S. MicroRNA-21 contributes to myocardial disease by stimulating MAP kinase signalling in fibroblasts. Nature. 2008; 456: 980-984.

3. Thum T, Fraccarollo D, Schultheiss M, Froese S, Galuppo P, Widder JD, Tsikas D, Ertl G, Bauersachs J. Endothelial nitric oxide synthase uncoupling impairs endothelial progenitor cell mobilization and function in diabetes. Diabetes. 2007; 56: 666-674.

4. Krutzfeldt J, Rajewsky N, Braich R, Rajeev KG, Tuschl T, Manoharan M, Stoffel M. Silencing of microRNAs in vivo with 'antagomirs'. Nature. 2005; 438: 685-689.

5. Frantz S, Fraccarollo D, Wagner H, Behr TM, Jung P, Angermann CE, Ertl G, Bauersachs J. Sustained activation of nuclear factor kappa B and activator protein 1 in chronic heart failure. Cardiovascular Research. 2003; 57: 749-756.

6. Kuehbacher A, Urbich C, Zeiher AM, Dimmeler S. Role of Dicer and Drosha for Endothelial MicroRNA Expression and Angiogenesis. Circ Res. 2007; 101: 59-68.

Downloaded from http://circ.ahajournals.org/ by guest on August 25, 2011

Supplemental Figures

Supplemental Figure 1

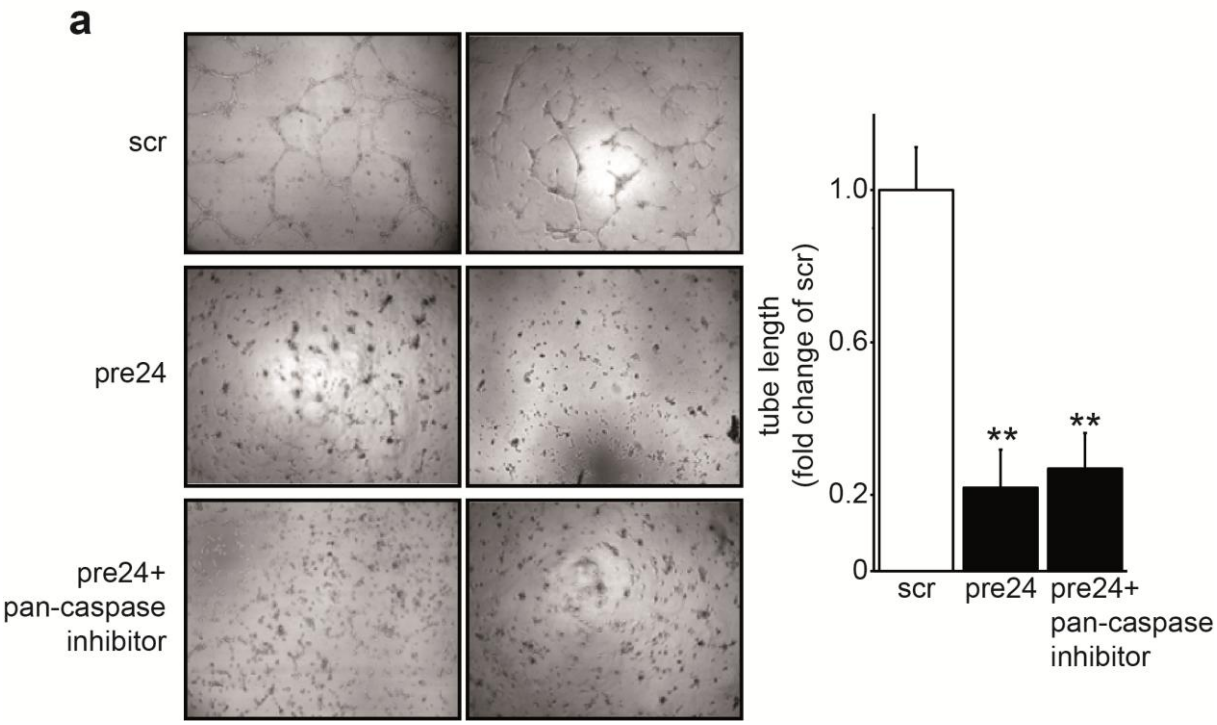

Downloaded from http://circ.ahajournals.org/ by guest on August 25, 2011

Supplemental Figure 2

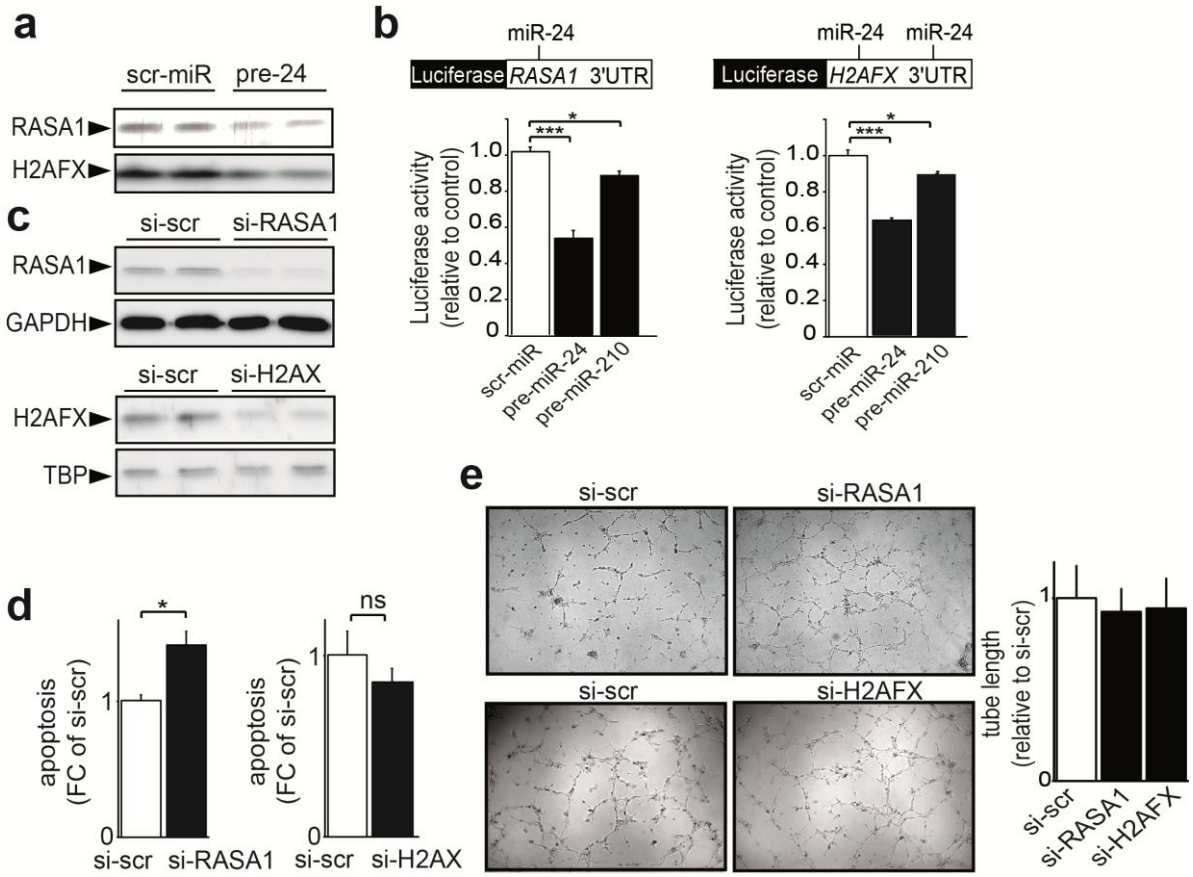

Downloaded from http://circ.ahajournals.org/ by guest on August 25, 2011

Supplemental Figure 3

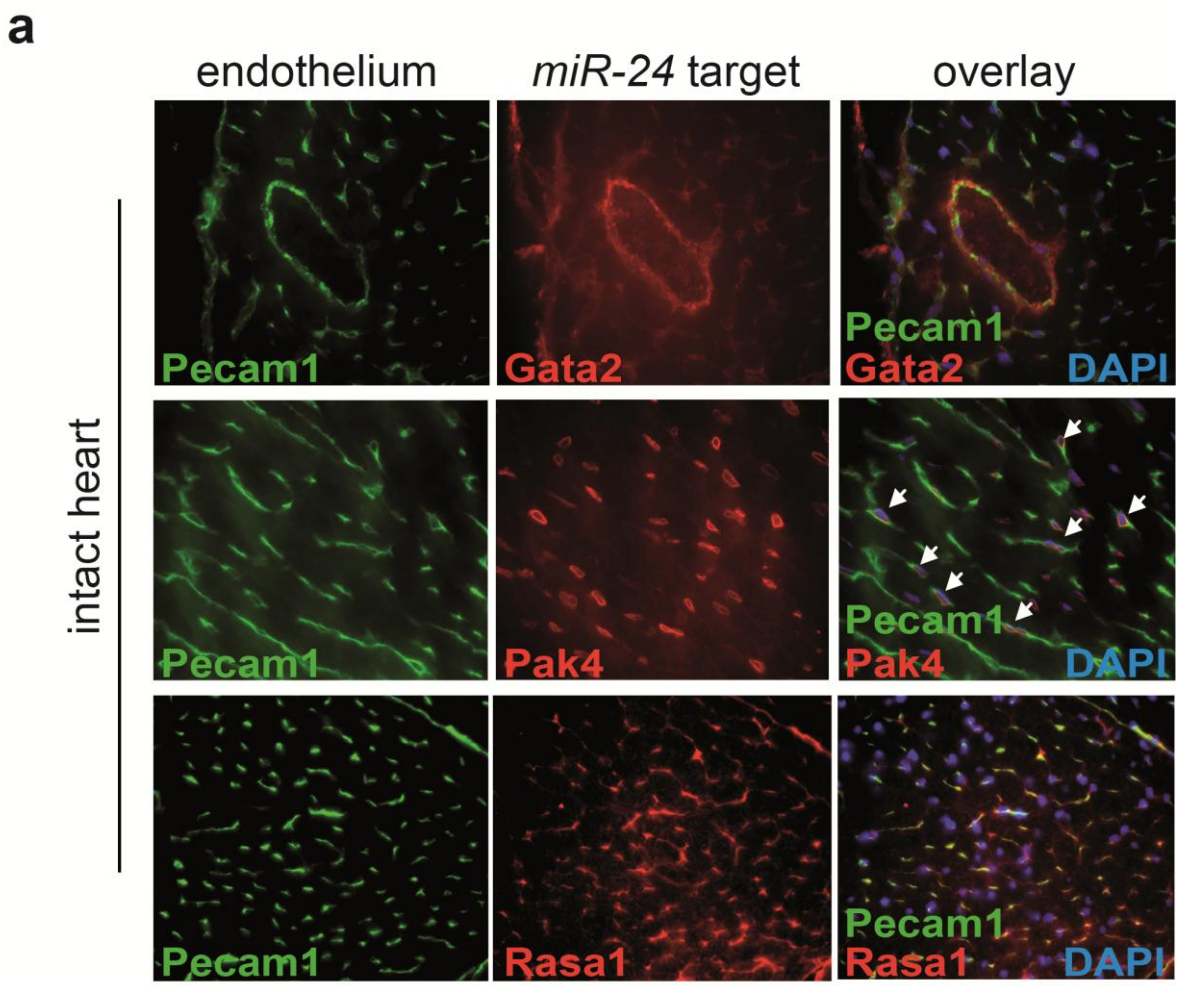

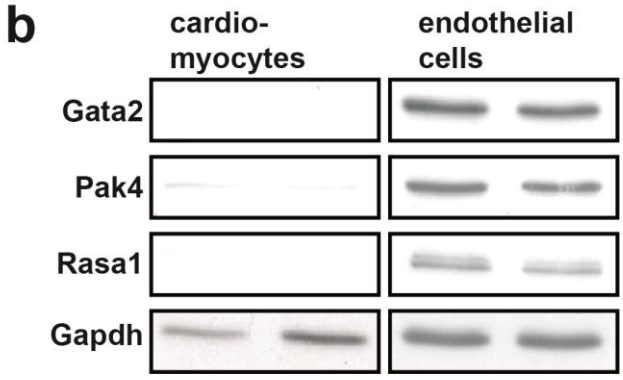

Downloaded from http://circ.ahajournals.org/ by guest on August 25, 2011

Supplemental Figure 4

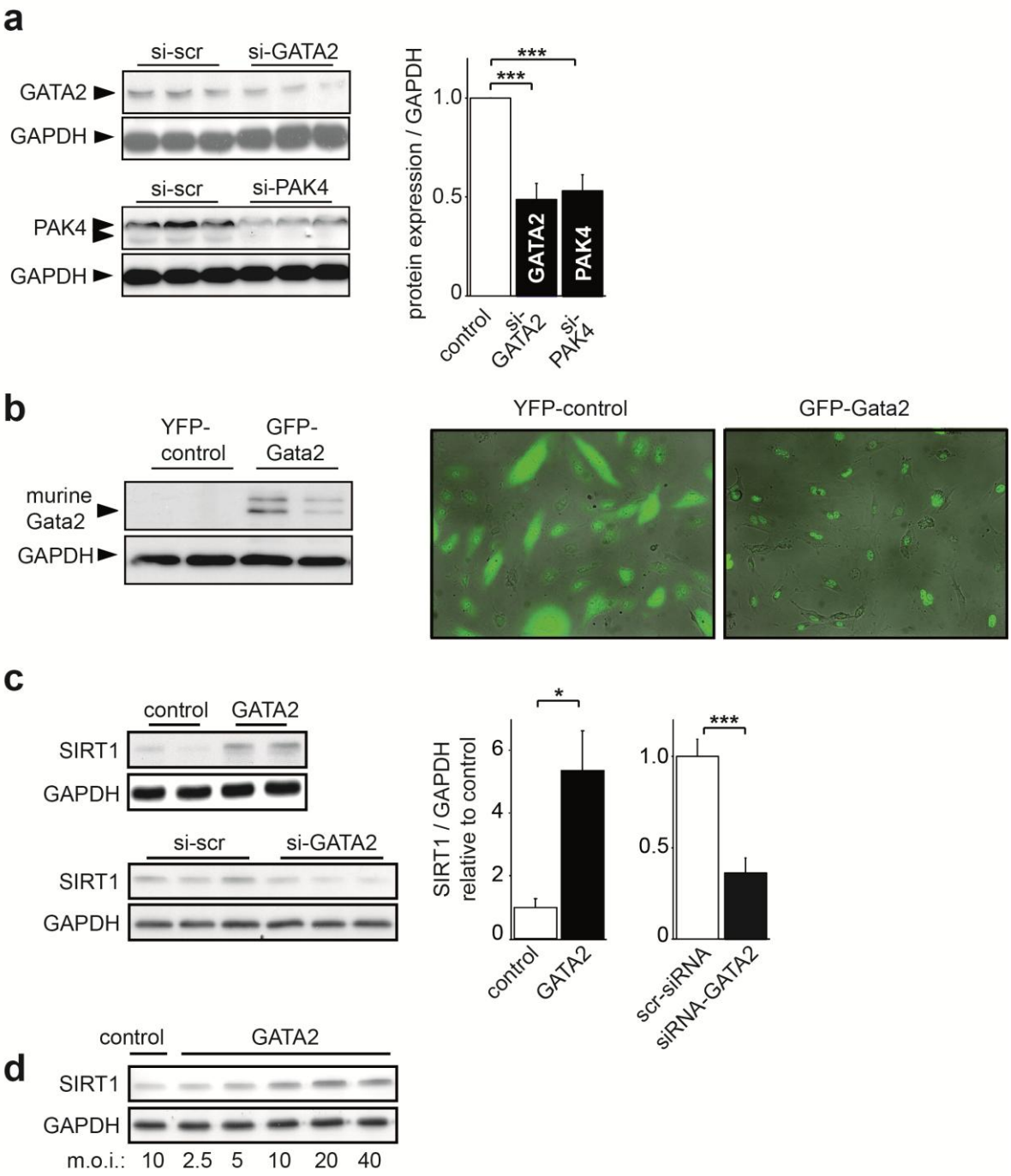

Downloaded from http://circ.ahajournals.org/ by guest on August 25, 2011

Supplemental Figure 5

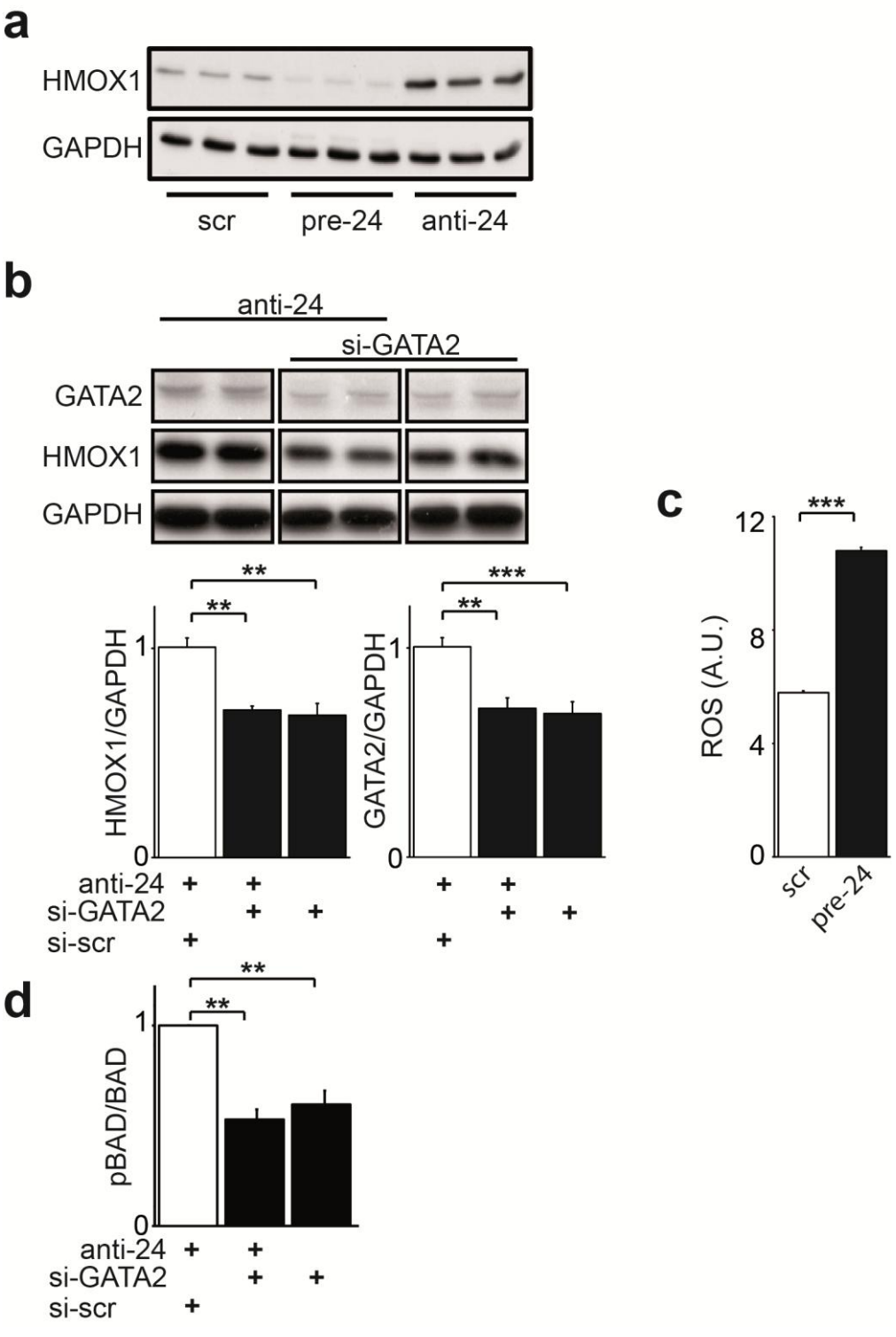

Downloaded from http://circ.ahajournals.org/ by guest on August 25, 2011

Supplemental Figure 6

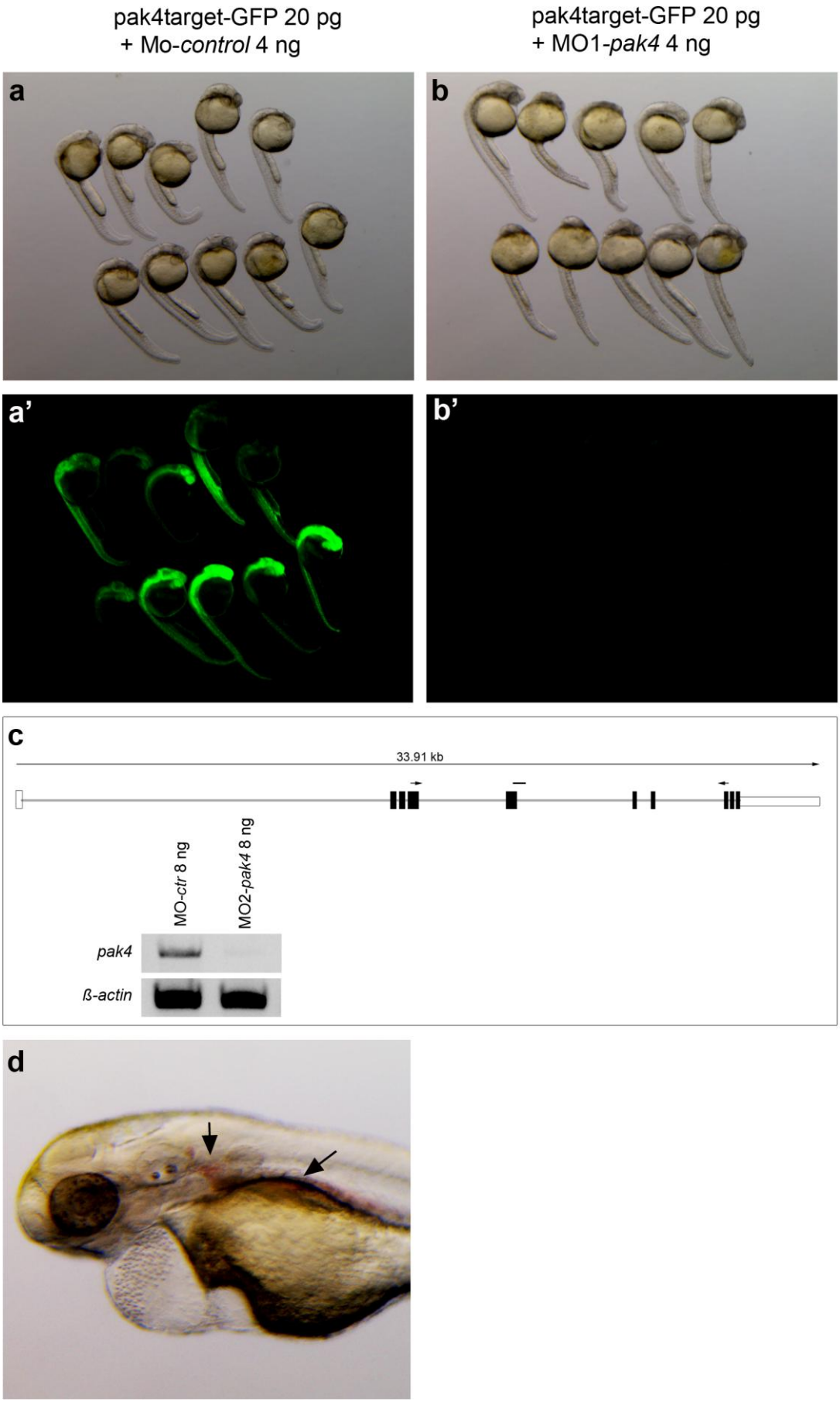

Downloaded from http://circ.ahajournals.org/ by guest on August 25, 2011

Supplemental Figure 7

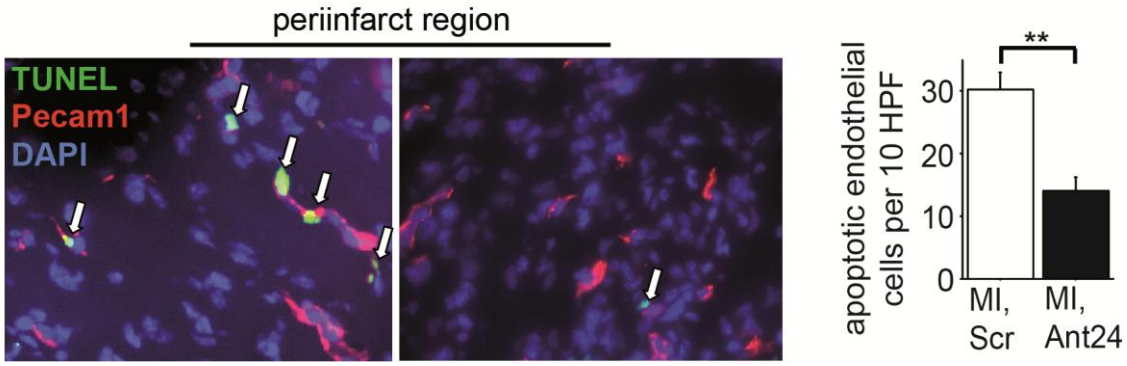

Downloaded from http://circ.ahajournals.org/ by guest on August 25, 2011